USGS
science for a changing world

Prepared in cooperation with the U.S. Army Corps of Engineers, Portland District

The Thermal Landscape of the Willamette River—Patterns and Controls on Stream Temperature and Implications for Flow Management and Cold-Water Salmonids

Scientific Investigations Report 2022–5035

U.S. Department of the Interior
U.S. Geological Survey

Cover. The Willamette River looking downstream, downstream from its confluence with the McKenzie River, near Coburg, Oregon. Photograph by Rose Wallick, U.S. Geological Survey, September 3, 2018.

The Thermal Landscape of the Willamette River, Oregon—Patterns and Controls on Stream Temperature and Implications for Flow Management and Cold-Water Salmonids

By Laurel E. Stratton Garvin and Stewart A. Rounds

Prepared in cooperation with the U.S. Army Corps of Engineers, Portland District

Scientific Investigations Report 2022–5035

U.S. Department of the Interior
U.S. Geological Survey

U.S. Geological Survey, Reston, Virginia: 2022

Suggested citation:
Stratton Garvin, L.E., and Rounds, S.A., 2022, The thermal landscape of the Willamette River—Patterns and controls on stream temperature and implications for flow management and cold-water salmonids: U.S. Geological Survey Scientific Investigations Report 2022–5035, 43 p., https://doi.org/10.3133/sir20225035.

Associated data for this publication:
Stratton Garvin, L.E., and Rounds, S.A., 2022, CE-QUAL-W2 models for the Willamette River and major tributaries below U.S. Army Corps of Engineers dams—2011, 2015, and 2016: U.S. Geological Survey data release, https://doi.org/10.5066/P908DXKH.

ISSN 2328-0328 (online)

Contents

Figures

Tables

Conversion Factors

U.S. customary units to International System of Units

Multiply	By	To obtain
	Length	
inch (in)	2.54	centimeter (cm)
foot (ft)	0.3048	meter (m)
mile (mi)	1.609	kilometer (km)
	Area	
square mile (mi^2)	2.590	square kilometer (km^2)
	Flow rate	
cubic foot per second (ft^3/s)	0.02832	cubic meter per second (m^3/s)

International System of Units to U.S. customary units

Multiply	By	To obtain
	Length	
kilometer (km)	0.6214	mile (mi)
	Area	
square kilometer (km^2)	0.3861	square mile (mi^2)
	Flow rate	
cubic meter per second (m^3/s)	35.31	cubic foot per second (ft^3/s)

Temperature in degrees Celsius (°C) may be converted to degrees Fahrenheit (°F) as:

$$°F = (1.8 \times °C) + 32.$$

Temperature in degrees Fahrenheit (°F) may be converted to degrees Celsius (°C) as:

$$°C = (°F - 32) / 1.8.$$

Abbreviations

°C	degrees Celsius
7dADMax	7-day average of the daily maximum
ESA	Endangered Species Act
JDAY	Julian day
RM	river mile
SI	International System of Units
USACE	U.S. Army Corps of Engineers
USGS	U.S. Geological Survey

The Thermal Landscape of the Willamette River, Oregon: Patterns and Controls on Stream Temperature and Implications for Flow Management and Cold-Water Salmonids

By Laurel E. Stratton Garvin and Stewart A. Rounds

Abstract

Water temperature is a primary control on the health, diversity, abundance, and distribution of aquatic species, but thermal degradation resulting from anthropogenic influences on rivers is a challenge to threatened species worldwide. In the Willamette River Basin, northwestern Oregon, spring-run Chinook salmon (*Oncorhynchus tshawytscha*) and winter-run steelhead (*O. mykiss*) are formerly abundant cold-water-adapted species that are now protected under the Endangered Species Act. Among the challenges to the health of cold-water salmonids in the Willamette River Basin, disruptions in the seasonal patterns of stream temperature imposed by 13 large, multipurpose dams on tributaries to the Willamette River, as well as temperatures routinely in excess of regulatory limits in the Willamette River Basin, are contributing factors. To better understand controls on stream temperature, the sensitivity of stream temperature to flow augmentation as a management tool for suppressing high temperatures, and the implications for threatened salmonids, this study used a two-dimensional hydrodynamic and water-quality model (CE-QUAL-W2) to investigate spatial and temporal patterns of stream temperature in the Willamette River Basin. This study focused on the upper 160.4 river miles of the Willamette River from the confluence of the Middle Fork and Coast Fork Willamette Rivers (river mile 187.2) to Willamette Falls (river mile 26.8), three representative climate years (2011, a cool and wet year; 2015, an extremely hot and dry year; and 2016, a moderately hot and dry year), and a series of flow-augmentation scenarios. Model results show that the Willamette River upstream from Willamette Falls is divisible into four characteristic "thermal reaches" with similar thermal patterns, depending on tributary input, warming rate, and the timing of thermal response. In general, the Willamette River warms downstream during spring and summer, but patterns are complex, influenced by tributary inflows, and seasonally variable. Except in cool wet years (as illustrated by 2011), modeling suggests that adversely warm conditions for spring-run Chinook salmon are extensive from June or July through August. The thermal influence of flow augmentation from dam storage on four tributaries with U.S. Army Corps of Engineers dams varies spatially along the Willamette River, seasonally, and in magnitude, depending on a range of factors like distance from the Willamette River, the temperature of dam outflow, and the thermal template of tributary reaches controlling stream temperature adjustment to environmental heat fluxes. Modeling suggests that targeted flow management (via augmentation from dam storage) can reduce the extent and duration of thermally stressful conditions for Chinook salmon for short periods, but modeling suggests that flow augmentation is limited in its ability to fundamentally alter the "thermal landscape" (the entire range of temperature variation in a river system over space and time) of the Willamette River. While this research provides general insights into the thermal landscape of the Willamette River and its sensitivity to flow management, additional investigation into the thermal landscape of tributaries downstream from U.S. Army Corps of Engineers dams, as well as the thermal management of reservoirs, storage availability, and dam outflows, would be necessary to target specific management actions for supporting specified rearing or migration conditions for spring-run Chinook salmon and other cold-water-adapted species in the Willamette River Basin.

Introduction

Water temperature is a primary control on the diversity, abundance, and distribution of riverine species (Vannote and others, 1980; Caissie, 2006; Webb and others, 2008). Many native fish species in the Willamette River Basin of northwestern Oregon are adapted to cold-water conditions, including spring-run Chinook salmon (*Oncorhynchus tshawytscha*) and winter-run steelhead (*O. mykiss*). These species were historically abundant but due to the cumulative effects of overfishing, pollution, habitat loss, and habitat degradation are now listed as threatened under the Endangered Species Act (ESA) of 1973 (Public Law 93–205, 87 Stat. 884, as amended; Sedell and Froggatt, 1984; National Marine Fisheries Service, 2008; Wallick and others, 2013). Among the challenges facing threatened fish populations in the Willamette Basin, thermal degradation is a major stressor (National Marine Fisheries

Service, 2008; Oregon Department of Fish and Wildlife and National Marine Fisheries Service, 2011). High stream temperatures have been shown to contribute to adult prespawn mortality, decreased growth and smoltification of juveniles, and increased predation and disease, while alterations to the magnitude and timing of the annual temperature patterns downstream from large dams have been shown to influence many aspects of aquatic life cycles, including egg survival, emergence, and out-migration (McCulloch, 1999; Caissie, 2006; Keefer and others, 2010; Olden and Naiman, 2010; Perry and others, 2015).

Thermal alteration resulting from large dams on tributaries to the Willamette River has long been recognized. The U.S. Army Corps of Engineers (USACE) owns and operates the Willamette Valley Project, which includes a system of 13 high-head (15 meters [m]) (International Commission on Large Dams, 2011) dams shown to modify the seasonality of the annual downstream temperature pattern, lagging both spring warming and autumn cooling as the combined result of thermal stratification and limited flexibility in the depth of release (Wetzel, 2001; Rounds, 2007; Sullivan and Rounds, 2004; Rounds, 2010; Olden and Naiman, 2010). To address these negative effects and mimic a more-natural seasonal temperature pattern downstream from Willamette Valley Project dams, USACE has pursued a variety of approaches, ranging from operational changes in dam releases to the planning and construction of temperature control towers designed to allow mixing of reservoir water from different depths prior to release (Buccola and others, 2012, 2015; Buccola, 2017; Rounds and Buccola, 2015). These efforts have shown some success in certain tributary reaches; however, the direct influence of temperature control on Willamette River Basin stream temperatures decreases with time and downstream distance as streams exchange heat with the surrounding environment (Rounds and Stratton Garvin, 2022).

The temperature of a stream is a dynamic balance between advective heat (the heat in water flowing from upstream or from groundwater, tributary, or human-derived inputs) and environmental energy fluxes (heat from solar and atmospheric radiation inputs, back radiation, conduction, evaporation, and condensation). As water travels downstream and river morphology and weather conditions change, the exchange of heat across the air-water and sediment-water interfaces causes the temperature to constantly adjust. The thermal response of a stream reach depends on the geology, groundwater discharge, topography, latitude, aspect, geomorphology, prevailing climate, anthropogenic factors like dams or urban areas, and other factors that influence stream heat content (Brown, 1969; Vannote and others, 1980; Bogan and others, 2003; Johnson, 2004; Tague and others, 2007; Burkholder and others, 2008). In the Willamette River, summer heating is constrained by flow augmentation from USACE reservoirs by (1) increasing the thermal mass in the river, which limits the temperature response to peak annual heating, and (2) decreasing the travel time (and thus exposure time to environmental energy fluxes) as water travels from the cooler foothills to warmer downstream reaches (Gregory and others, 2007b; Risley and others, 2010; Rounds, 2010; Wallick and others, 2013; Stratton Garvin and others, 2022b). In recognition of thermal and ecosystem benefits, USACE manages the system of dams in the Willamette River Basin to meet or exceed minimum streamflow levels at Albany, Salem, and at selected tributary sites, as prescribed by a 2008 Biological Opinion (National Marine Fisheries Service, 2008).

Although the influence of dam releases, the relation between streamflow and stream temperature, and patterns of downstream warming are understood for the Willamette River in a general way, much remains unknown about the thermal conditions and the effects of various hydroclimatological conditions and management actions on stream temperatures throughout the river system. This study uses results from CE-QUAL-W2, a two-dimensional hydrodynamic and water-quality model, to investigate the "thermal landscape" (the entire range of temperature variation in a river system over space and time) (Fullerton and others, 2015; Steel and others, 2017) of conditions in the Willamette River. By comparing the modeled stream temperature of the Willamette River in four empirically designated "thermal reaches" (a river reach of varying length with similar thermal patterns) for three representative climate years (2011, a cool and wet year; 2015, an extremely hot and dry year; and 2016, a moderately warm and dry year) across a series of flow-augmentation scenarios in major, dam-controlled tributaries to the Willamette River, this study provides insight into the controlling factors influencing stream temperature in the Willamette River and into potential actions to improve thermal conditions for threatened fish populations in the Willamette River Basin.

Study Area Description

The Willamette River is the principal stream draining the 11,500 square mile (mi^2) Willamette River Basin in northwestern Oregon (fig. 1). Flowing approximately 187 miles north from its start at the confluence of the Coast Fork Willamette and Middle Fork Willamette Rivers to its confluence with the Columbia River, the Willamette River receives inflow from three distinct regions of the basin: the Coast Range to the west, the Cascade Range to the east, and the fertile Willamette Valley, which is home to Oregon's largest cities, including Eugene, Corvallis, Albany, Salem, and Portland, and one of the most diverse agricultural regions in the state (Conlon and others, 2005).

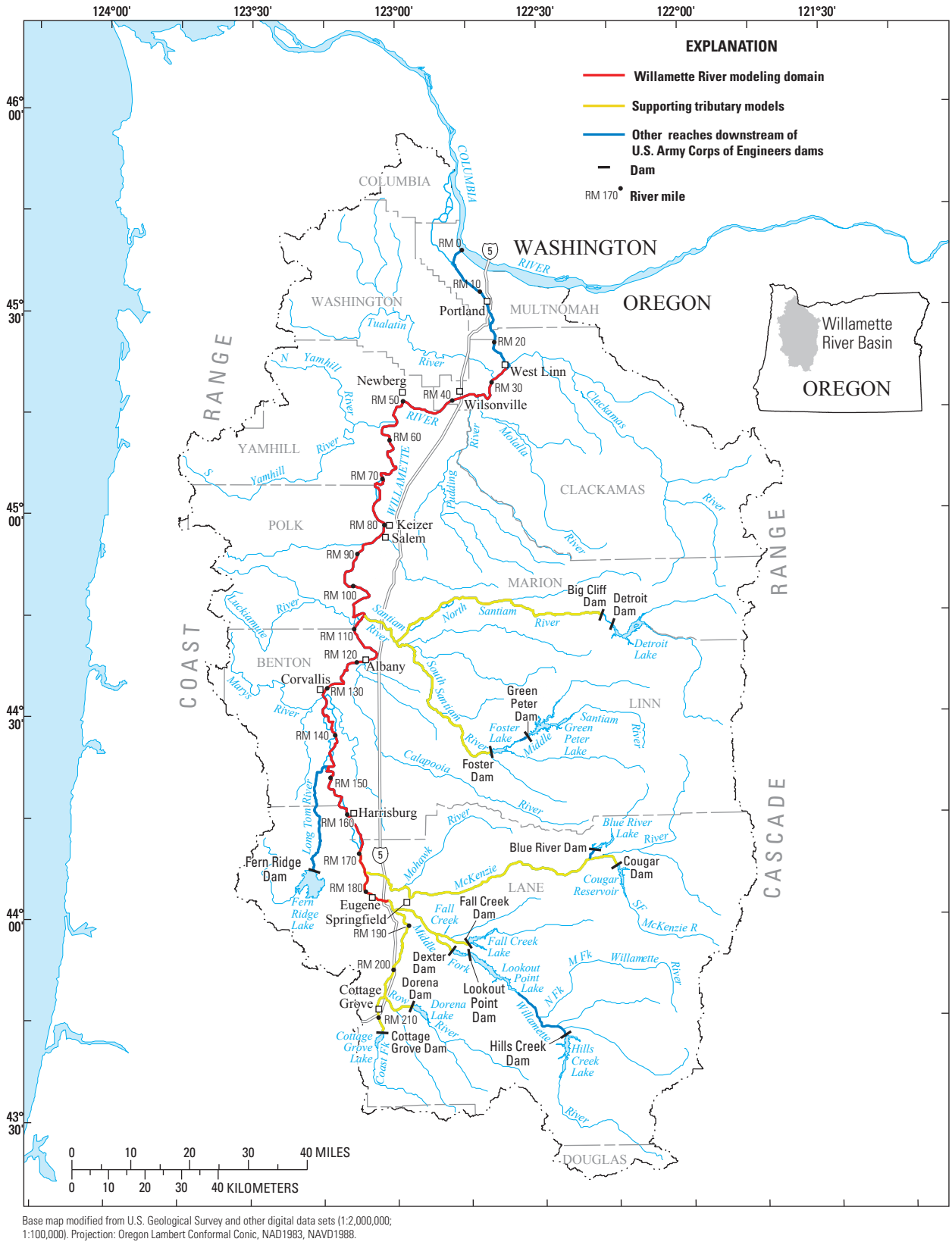

Base map modified from U.S. Geological Survey and other digital data sets (1:2,000,000; 1:100,000). Projection: Oregon Lambert Conformal Conic, NAD1983, NAVD1988.

Figure 1. Map showing the Willamette River Basin in northwestern Oregon, showing the Willamette Valley Project dams and reservoirs and the river reaches modeled in this study. Map modified from Stratton Garvin and others (2022b).

The geomorphic character of the Willamette River varies along its length and has been influenced by many substantial anthropogenic actions over at least the last 150 years (Wallick and others, 2007; Wallick and others, 2013). While predominantly a single-thread, gravel-bedded river, in its upper reaches, from the confluence of the Coast Fork Willamette and Middle Fork Willamette Rivers (river mile [RM] 187) to Corvallis (RM ~131), the Willamette River was historically more dynamic than downstream reaches and presently has numerous actively shifting gravel bars and side channels with active migration processes and occasional multi-thread sections (Wallick and others, 2013). In contrast, from Corvallis to the confluence of the Willamette and Santiam Rivers (RM 109), side channels and actively shifting bars are relatively rare. Downstream from the Santiam River confluence to the head of the Newberg Pool (RM 50), the Willamette River is geomorphically stable, with low historical rates of meander migration and avulsions, but has more and larger gravel bars and abundant secondary channels as compared to the reach from Corvallis to the Santiam River confluence. The "Newberg Pool," a reach extending from approximately RM 50.0 to Willamette Falls at RM 26.8, is a bedrock-constrained, deep, low-gradient reach pooled by the falls at its downstream boundary (Dykaar and Wigington Jr., 2000). Willamette Falls is a 40-foot (ft) high, river-spanning basalt intrusion which, prior to the installation of locks and other modifications, created a barrier to both navigation and low-flow fish passage (Oregon Department of Fish and Wildlife and National Marine Fisheries Service, 2011; National Marine Fisheries Service, 2008). The Willamette River downstream from Willamette Falls (often referred to as the "lower Willamette River") is tidally influenced to its confluence with the Columbia River north of the city of Portland.

Prior to European settlement, the Willamette River Basin supported large populations of anadromous fish. Although no direct estimates of anadromous fish runs prior to the 1940s exist, anecdotal evidence suggests that spring-run Chinook salmon may have been as high as 275,000 fish in the 1920s (Myers and others, 2006); others estimate that the upper Willamette River Basin may have supported millions of salmonids prior to the onset of habitat degradation and other stressors in the early 1800s (Oregon Department of Fish and Wildlife, The State of Oregon, and the National Oceanic and Atmospheric Administration, 2011). The primary natal streams for these fish populations all drain the western slopes of the Cascade Range, and include the Clackamas, Molalla, Santiam, Calapooia, McKenzie, and Middle Fork Willamette Rivers and their tributaries. Both juvenile and adult salmonids have been documented in streams draining the Coast Range; for example, the Coast Fork Willamette, Marys, and Long Tom Rivers, but these streams are not thought to have supported large populations of anadromous fish (Myers and others, 2006; Oregon Department of Fish and Wildlife and National Marine Fisheries Service, 2011). Following centuries of decline, Upper Willamette River spring-run Chinook salmon and Upper Willamette River winter-run steelhead were listed as threatened under the ESA in 1999 (National Marine Fisheries Service, 1999a, 1999b).

Streamflow in the Willamette River and its tributaries is influenced by seasonal weather patterns, by the geology and physiography of tributary sub-basins, and by flow management operations at large, multi-purpose dams on tributaries in the basin. Pacific Ocean-derived, eastward-moving storms provide most of the precipitation to the basin, which typically falls as rain in the Coast Range, Willamette Valley, and lower Cascade Range foothills, and as snow along the crest of the Cascade Range. Most precipitation falls between October and March; annual totals vary with elevation, ranging from approximately 35-40 inches in the valley lowlands up to 130 inches or more along the crest of the Coast and Cascade Ranges (Wentz and others, 1998; PRISM Climate Group, 2020). In general, the largest streamflows are the result of winter storms, whereas the lowest streamflows occur in late summer prior to the start of the autumn rainy season. However, for tributaries deriving water from the High Cascades, a region dominated by young, highly permeable basalts, this pattern is moderated by abundant groundwater contributions to streamflow and by winter storage of precipitation as snow in the upper elevations of the basin (Conlon and others, 2005; Tague and Grant, 2004; Jefferson and others, 2006). A substantial proportion of streamflow in the Willamette River is controlled by USACE through its operation of 13 tributary dams, used to mitigate flood risk hazards to downstream communities and provide hydropower, navigation, water supply, and ecological and other benefits. Water stored during winter is used to augment summer streamflow in the Willamette River, with augmented streamflow at Salem about double the historical low-flow average (U.S. Geological Survey continuous monitoring site 14191000; Rounds, 2010; U.S. Geological Survey, 2020).

Stream temperatures in the Willamette River system generally follow seasonal climate patterns but vary spatially according to elevation, geology, geomorphology, and in response to anthropogenic influences. Tributaries with significant inputs from the High Cascades tend to be cold and thermally stable, with muted warming both seasonally and downstream as compared to stream reaches without significant groundwater inputs (Tague and others, 2007; Rounds, 2010). In contrast, streams draining the Coast Range and lower-elevation Western Cascades, which are dominated by rainfall-derived runoff and naturally lower summer base flows, tend to be warmer and more responsive to seasonal thermal loads (Tague and others, 2007; Dent and others, 2008; Leach and others, 2017; U.S. Geological Survey, 2020). These general patterns, however, are influenced by geomorphic characteristics that control the degree of shading, riparian vegetation, hyporheic flow, and stream velocity of individual reaches; additionally, anthropogenic influences like dam operations, water withdrawals for irrigation and municipal use, and point source discharges all influence local stream temperature and downstream thermal adjustments. The temperature effects of dam releases on downstream reaches in the Willamette

River Basin have been modeled to be as large as 6.0 – 6.5 °C (both warmer and cooler, depending on a range of factors); however, management actions implemented since 2005 have shown some success in reducing the magnitude of these effects (Rounds 2007; Sullivan and Rounds, 2004; Rounds, 2010; Hansen and others, 2017).

Hydrology and Geomorphology of Tributaries Downstream from U.S. Army Corps of Engineers Dams with Historical Salmonid Populations

Of the USACE-dammed tributaries to the Willamette River with historical populations of salmonids, the Santiam River Basin provides the most reservoir storage. The South Santiam River is dammed by Foster Dam, 36.4 miles upstream from the South Santiam-North Santiam River confluence (48.3 miles from the Willamette River), and Green Peter Dam farther upstream on the Middle Santiam River (fig. 1). Together, these reservoirs comprise approximately 28 percent of total available conservation storage in the Willamette Valley Project (National Marine Fisheries Service, 2008). The North Santiam River is dammed by Big Cliff Dam and Detroit Dam immediately upstream. Big Cliff Dam, located approximately 58.6 miles upstream from the Willamette River, has negligible storage but regulates outflow from Detroit Dam, a large flood-risk management dam that provides approximately 16 percent of total conservation storage in the Willamette Valley Project (National Marine Fisheries Service, 2008). The South Santiam River drains a region dominated by relatively steep, dissected, and impermeable Western Cascades geology and has an average slope of 0.1321 percent (Wallick and others 2013; Risley and others, 2012). In contrast, the North Santiam River drains a basin dominated by High Cascades geology. With an average slope of 0.28 percent and relatively limited channel stabilization, the North Santiam River is both the steepest and most dynamic of the USACE-dammed Willamette River tributaries (Wallick and others, 2013). From non-alluvial reaches in the steeper canyons downstream from the major dams, both the North Santiam and South Santiam Rivers transition to predominately alluvial domains in their lower elevations. In contrast to the North Santiam River, both the South Santiam and Santiam Rivers are predominantly single-thread and have been extensively stabilized by revetments (Wallick and others, 2013).

The McKenzie River is a major tributary to the Willamette River that is characterized by stable, spring-fed streamflows that originate in its upper basin, and includes extensive water management projects. The Eugene Water and Electric Board operates a hydropower complex and two hydropower canals on the McKenzie River, which significantly alter streamflow (Risley and others, 2010). Flood-risk management dams include Cougar Dam on the South Fork McKenzie River and Blue River Dam on Blue River, a tributary to the McKenzie River. Blue River Dam impounds a relatively small reservoir (4 percent of total available Willamette Valley Project conservation storage), whereas Cougar Dam impounds approximately 8 percent of total available Willamette Valley Project conservation storage. Cougar Dam, located 60.7 river miles upstream from the Willamette River, has a selective withdrawal tower which has operated to moderate the temperature of dam releases since 2005 (Rounds, 2007). The South Fork McKenzie and McKenzie Rivers are relatively steep downstream from Cougar Dam, with an average slope of 0.19 percent (Wallick and others, 2013). The McKenzie River is narrow and steep in its upper reaches but occupies a wide alluvial corridor in its lower reaches (Risley and others, 2010).

The Middle Fork Willamette River is the final major, USACE-dammed tributary with historical salmonid populations. USACE operates four major dams in the Middle Fork Willamette River Basin. On the Middle Fork Willamette River, Dexter Dam is 16.5 miles upstream and serves as a re-regulation dam for Lookout Point Dam, which impounds the largest reservoir by volume in the Willamette Valley Project (18 percent of total available conservation storage). Farther upstream, the reservoir impounded by Hills Creek Dam comprises 14 percent of available conservation storage. Additional storage in the Middle Fork Willamette River Basin is provided by Fall Creek Dam (impounding 6 percent of available Willamette Valley Project conservation storage) on Fall Creek, a tributary that joins the Middle Fork Willamette River downstream from Dexter Dam. The Middle Fork Willamette River downstream from Dexter Dam has an average slope of 0.219 percent but is largely laterally stable, due to the decrease in peak flows and bed-material supply, encroachment of forest vegetation and enhanced bank protection (Wallick and others, 2013, 2018).

Management and Hydroclimatological Conditions in Modeled Years

The analysis in this report is based on modeled stream temperatures in March through October of 2011, 2015, and 2016. These years were chosen as a representation of the range of recent conditions measured in the Willamette River (fig. 2; table 1). Air temperature in 2011 was characterized by a “near normal” winter followed by the second coldest spring (calculated as April through June) on record in the Willamette Valley (table 1; National Oceanic and Atmospheric Administration National Centers for Environmental Information, 2020). Precipitation was average in winter, followed by an above-normal spring (calculated as April through June) and a below normal summer (calculated as July through September) and autumn (calculated as October through December). In contrast, 2015 was the hottest year on record (1895–2020) in the Willamette Valley, defined by the record warmest winter and top decile spring, summer, and autumn. Until autumn, 2015 was also very dry, with below-average or much-below-average precipitation in the winter, spring, and summer. Compared to 2015, 2016 represents less extreme air temperature and precipitation conditions; however, conditions from winter

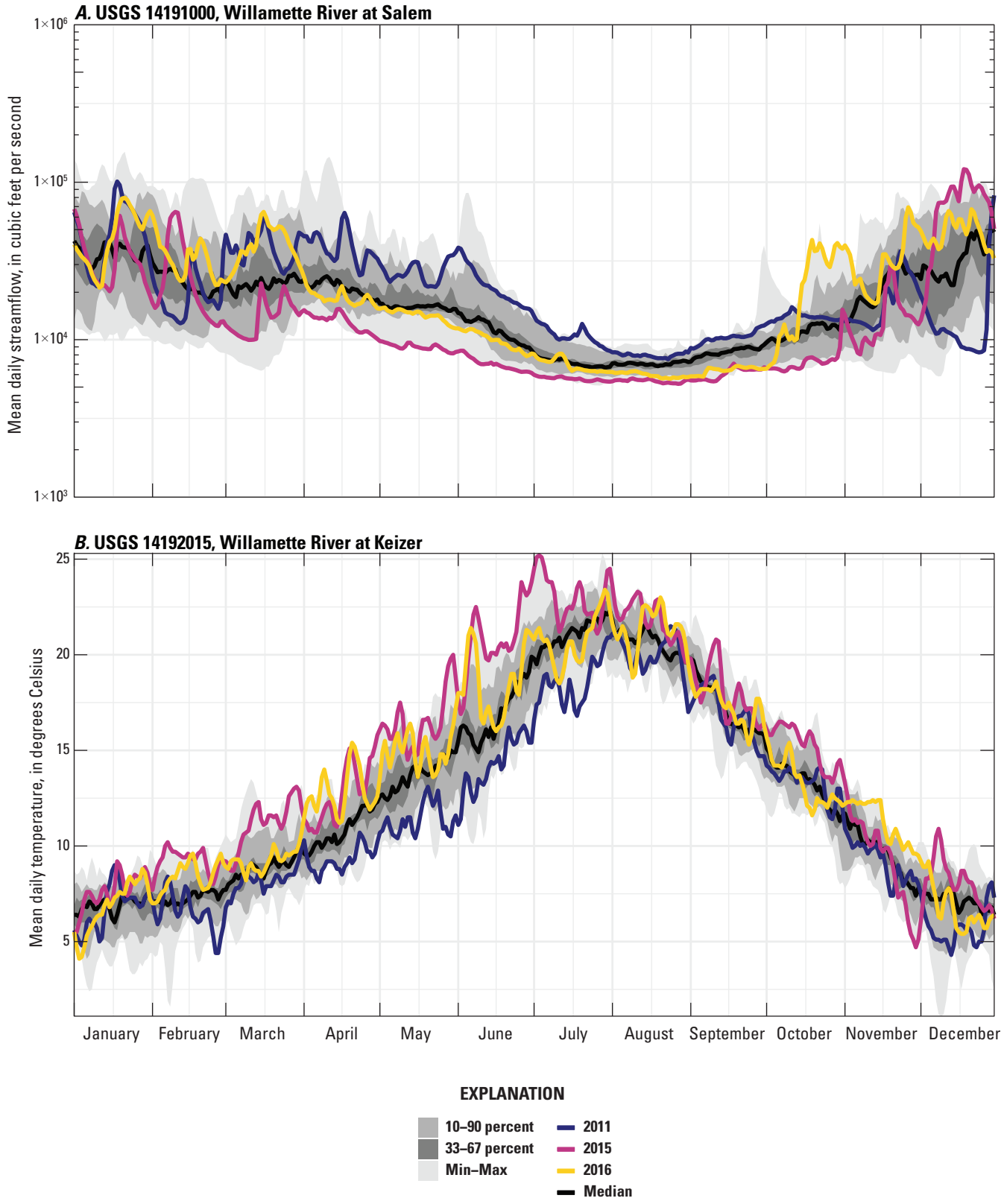

Figure 2. Range of (*A*) streamflow and (*B*) water temperature conditions in the Willamette River at Salem (USGS station 14191000) and Keizer (USGS station 14192015), northwestern Oregon. Percentiles were computed using measurements from January 2001 through December 2020 (U.S. Geological Survey, 2020). USGS, U.S. Geological Survey.

Table 1. Seasonal and annual air temperature and precipitation divisional rankings for the Willamette Valley, northwestern Oregon, 1895–2020.

[For a period of 126 years, a ranking of 1 represents the coolest or driest conditions on record, whereas a ranking of 126 represents the warmest or wettest conditions on record. Colors correspond to the categorization scheme utilized by the National Oceanic and Atmospheric Administration, where the upper and lower tercile are considered "above/below normal," the middle tercile is considered "near normal," and the upper and lower deciles are considered "much above/much below normal." Data from National Oceanic and Atmospheric Administration National Centers for Environmental Information (2020).]

Period	Rank					
	Average air temperature			Average precipitation		
	2011	*2015*	*2016*	*2011*	*2015*	*2016*
January–March	58	126	121	74	17	78
April–June	2	122	125	115	7	23
July–September	93	121	96	25	38	33
October–December	37	114	76	25	111	115

Key	Average air temperature	Average precipitation
Record		
1–13 = Much below normal		
14–42 = Below normal		
43–84 = Near normal		
85–113 Above normal		
114–126 Much above normal		
Record		

through summer of 2016 were also predominantly warm and dry (table 1). The Willamette Valley Project did not reach full storage capacity in either 2015 or 2016, with reservoir levels often lower in 2015 than in 2016 (U.S. Army Corps of Engineers, 2020). All three modeled years are representative of "modern" operations in the Willamette Valley Project, with streamflows managed to comply with the requirements of the 2008 Willamette River Basin Flood Control Project Biological Opinion (National Marine Fisheries Service, 2008) and dam releases managed for temperature at Cougar Dam, where a temperature control tower was completed in 2005, and at Detroit Dam, where operational changes instituted in 2007 improved the downstream thermal regime (Risley and others, 2010; Rounds, 2010).

Purpose and Scope

This report documents an analysis of spatial and temporal stream temperature patterns in the Willamette River in 2011, 2015, and 2016, the potential effect of thermal conditions on threatened cold-water salmonids in selected rivers of the Willamette River Basin, and the sensitivity of stream temperature to additional flow augmentation. All analyses of water temperature were completed using CE-QUAL-W2, a two-dimensional water-quality model with a long history of usage in the Willamette River Basin and elsewhere (Wells, 2019; Stratton Garvin and others, 2022b, and references therein). Analyses use the modeled daily mean or daily maximum temperature for each model segment and literature-derived life-stage-specific temperature thresholds for Upper Willamette River spring-run Chinook salmon (White and others, 2022) to develop a series of metrics and visualizations characterizing the temporal and spatial variability of stream temperature in the Willamette River. Temperature thresholds for both juvenile and adult Chinook salmon are presented but the majority of the analysis focuses on juvenile Chinook salmon.

Modeling Domain and Flow-Augmentation Scenarios

The modeling in this report was completed using six previously developed CE-QUAL-W2 Willamette River Basin submodels of the Coast Fork Willamette, Middle Fork Willamette, McKenzie, South Santiam, North Santiam, and Santiam Rivers, as well as the upper and middle section of the main-stem Willamette River, as defined by Stratton Garvin and others (2022b; fig. 1). These submodels extended upstream as far as the lowermost USACE dam on a given tributary and were linked together to run as a single, integrated model. The model domain included streams downstream from all USACE dams in the Willamette River Basin except for the Long Tom

River downstream from Fern Ridge Dam and Blue River (a tributary to the McKenzie River) downstream from Blue River Dam, which either do not have existing CE-QUAL-W2 models (Blue River) or are considered a lower modeling priority by USACE (Long Tom River). Except where referenced to a specific measured dataset, "baseline conditions" refer to model results produced using measured or estimated data to simulate measured river temperatures from March 24 or 23 (in 2016, a leap year) through October 30 or 31.

The primary analytical focus of this report is on the Willamette River itself, defined here as the main channel of the Willamette River from RM 187.2 at the confluence of the Coast Fork Willamette and Middle Fork Willamette Rivers, to RM 26.8 at Willamette Falls. However, all model results, including both baseline conditions and flow-augmentation scenarios, were modeled using the full Willamette River system modeling domain as defined by Stratton Garvin and others (2022b), which included rivers in the Middle Fork Willamette, Coast Fork Willamette, McKenzie, and Santiam River Basins. Flow-augmentation scenarios included the addition of a total of 1,000 cubic feet per second (ft^3/s) to the baseline conditions for the duration of the model simulation in 2011, 2015, and 2016 as hypothetically released from one upstream dam at a time on the Middle Fork Willamette, McKenzie, North Santiam, or South Santiam Rivers, for a total of 12 scenarios. Limited analysis from the outflow of tributary submodels was used to investigate reasons for the difference in flow-augmentation influence on Willamette River temperatures, but detailed analysis of results from the tributary submodels themselves was beyond the scope of this study.

This report is intended to describe patterns and controls on stream temperature in streams of the Willamette River Basin downstream from USACE dams. A basic level of literacy in modeling and stream temperature dynamics is assumed. For more in-depth information about stream temperature dynamics, stream temperature modeling, and previous work in the Willamette River Basin, readers may consult foundational texts, reviews, and other supporting documents, including Brown (1969), Poole and Berman (2001), Caissie (2006), Rounds (2010), Wells (2019), Stratton Garvin and others (2022a, 2022b), and Rounds and Stratton Garvin (2022).

Locations and Reporting Units

Locations along the Willamette River and its tributaries are referred to by RM for river mile, which starts at the mouth of each stream or river and measures the centerline distance upstream. The RMs used in this report were calculated using the underlying CE-QUAL-W2 model geometry and then aligned with locations in the real world (such as confluences or gaging stations) using the location of Willamette Falls, at RM 26.76, and the original model documentation as references (Stratton Garvin and others, 2022b). Because the CE-QUAL-W2 model grid was somewhat simplified and because the river has continued to meander across its floodplain in some reaches, the RMs reported here may not align with those reported by other sources.

Other units of measurement utilized in this report reflect the mixed International System (SI) of Units and U.S. Customary Units used by floodplain managers of the Willamette River Basin. Streamflow is presented in cubic feet per second (ft^3/s) to align with the standard language used by dam operators, USGS streamflow gaging station measurements, and streamflow requirements established in the Biological Opinion (National Marine Fisheries Service, 2008). Temperature is reported in degrees Celsius (°C). Unit conversions are presented in the report front matter.

Methods

CE-QUAL-W2 is a two-dimensional, process-based hydrodynamic and water-quality model with a long history of application in the Willamette River Basin (Wells, 2019; Stratton Garvin and others, 2022b, and references therein). Designed for use in long, narrow water bodies that may stratify (such as lakes and reservoirs), models built in CE-QUAL-W2 are depth and longitudinally discrete but laterally averaged. CE-QUAL-W2 calculates water movement from the balance of frictional and gravitational forces within the framework of the model grid, a three-dimensional estimate of stream or reservoir bathymetry, inflows, outflows, and structural features specific to the individual model domain. Stream temperature is calculated using a heat budget based on the net balance of environmental and advective energy fluxes and includes a dynamic representation of topographic and vegetative shading (Wells, 2019). Models built with CE-QUAL-W2 are most appropriately built at the "reach-scale" (as opposed to a larger "basin scale" or smaller "habitat scale"), with the length of each model segment (the model discretization unit in the longitudinal, or upstream-downstream direction) and the height of each layer (the model discretization unit in the z, or vertical, direction) developed to provide results that are (1) grid-independent (model output is not a function of how the underlying bathymetric grid is constructed) and (2) computationally feasible (run times and required computing power are reasonable and within the computing capabilities of the computer system in use). CE-QUAL-W2 can be configured to run a single simulation for as long a simulated time period as is computationally feasible. The simulation timestep, with some user-based controls, is internally computed by CE-QUAL-W2 based on mass conservation and numerical stability constraints, but the output frequency is user designated.

The submodels used in this analysis are a subset of those that were originally developed to support the establishment of a Total Maximum Daily Load for water temperature in the Willamette River and selected tributaries by simulating conditions in the summers of 2001 and 2002 (Annear and others, 2004; Berger and others, 2004; Sullivan and Rounds, 2004; Bloom, 2016). The submodels were subsequently updated to CE-QUAL-W2 version 4.2 and configured to simulate conditions from day-of-year (JDAY; after "Julian day") 80 (March 21st in a non-leap year) to JDAY 305 (November 1

in a non-leap year) of 2011, 2015, 2016 (Stratton Garvin and others, 2022b). Although the exact dimensions varied within and between submodels, in general, the submodels used in this study were discretized to segment lengths on the order of 100–500 m and layer heights of approximately 0.4–1.0 m. Statistical measures of model fit have shown that the models are capable of simulating subdaily stream temperatures with a mean absolute error of generally less than 1 °C and often near 0.5 °C, with minimal bias. Further details on model improvements, updates, and fit are described by Stratton Garvin and others (2022b). All baseline condition models and scenarios as well as the model computer code are available from Stratton Garvin and Rounds (2022). All analyses were derived from the model-calculated, flow-weighted daily mean or daily maximum temperature for each segment in the model domain ("FlowTemp.dat," a customized output from CE-QUAL-W2). All subsequent analysis was performed using the R statistical package (R Core Team, 2020).

Analyses were based on temperature thresholds for Chinook salmon from White and others (2022), based on a literature review utilizing numerous sources including Brett (1982), McCullough (1999); Marine and Cech, Jr. (2004), and Perry and others (2015). Thermal categories include "lethal," "adverse," "optimal," and "suboptimal" as a description of their likely effect on the fish of the specified life stage. Categories are derived from two sets of thresholds, one set for juvenile rearing and growth and a separate set for adult migration, and are based on the daily mean water temperature (table 2). The available thresholds are limited to juvenile rearing and adult migration of Chinook salmon, but future analysis may make use of similar thresholds for adult Chinook salmon spawning and for multiple life stages of steelhead.

Flow-sensitivity scenarios were performed by uniformly adjusting the measured dam-release flow rates to the upstream end of the models in question, including the Coast Fork Willamette, Middle Fork Willamette, McKenzie, South Santiam, North Santiam, and Santiam River models. These flow sources were selected to represent reservoirs with large storage capacities on tributaries with current or historical populations of threatened anadromous fish. A total of twelve scenarios were simulated by adjusting the measured inflow to the South Santiam, North Santiam, South Fork McKenzie, or Middle Fork Willamette Rivers by a uniform addition of 1,000 ft^3/s (28.3 m^3/s in the model) to the baseline inflow for the entire model duration for all three model years. This addition resulted in a percent increase in streamflow ranging from 2.5 to 27.7 percent at Albany (upstream from the Santiam River confluence) and 1.62 to 19.5 percent at Salem (downstream from the Santiam River confluence), depending on the year and seasonal variation (app. 1, fig. 1.1). No attempt to calculate available storage volumes or produce a realistic flow regime were attempted, as this exercise was intended to investigate the sensitivity to flow management of the Willamette River rather than to suggest an operational flow-management regime.

Additionally, for simplification, no effort to adjust the temperature of dam releases was attempted for any scenario. As with flow, this exercise was not intended to suggest actual changes to dam operations regarding the temperature of dam releases, and such a detailed, operationally based analysis is beyond the scope of this investigation. This simplification is unrealistic, as an increase or decrease in dam releases would change the internal thermal structure of the reservoir upstream, thus altering the temperature of the outflow. Some specific implications of this simplification are discussed in subsequent sections of this report; however, because the direct thermal influence of dam-release temperatures decreases with distance downstream as heat is exchanged with the surrounding environment, this approach is generally reasonable for results in the Willamette River (Rounds, 2010; Rounds and Stratton Garvin, 2022).

Table 2. Water temperature thresholds and their potential effect on Chinook salmon (*Oncorhynchus tshawytscha*) during juvenile rearing and growth or adult migration, Willamette River, northwestern Oregon.

[Thresholds are designated based on the daily mean temperature, in degrees Celsius. **Category name** is used in figures 7, 8, and 13. **Abbreviations**: °C, degrees Celsius; ≥, greater than or equal to; <, less than; ≤ less than or equal to]

Juvenile rearing and growth		Adult migration		Category name
Temperature range (°C)	Effects on fish	Temperature range (°C)	Effects on fish	
≥ 24 °C	Mortality	≥ 23 °C	Mortality	Lethal
≥20–24 °C	Sub-optimal due to increased stress, decreased growth and potential for disease	≥19–23 °C	Migration impaired	Adverse
≥10–20 °C	Optimal	≥12–19 °C	Optimal	Optimal
<10 °C	Safe, but decreased growth	<12 °C	Safe, preferred for spawning	Suboptimal

Results

The "thermal landscape" (after Fullerton and others, 2017) of a river system describes the entire range of temperature variation in a river system over time and space. To adequately characterize the thermal landscape, a number of metrics must be used. Temporal variation, or the "thermal regime" of a river system, can be assessed in terms of (1) magnitude, (2) duration, (3) frequency, (4) timing, and (5) variability or rate of change (after Olden and Naiman, 2010; Steel and others 2017). Because the thermal landscape considers variation of a thermal regime in both time *and* space, it is also necessary to assess (1) location, (2) scale, (3) extent, and (4) heterogeneity. The appropriate metrics applied to these components of temperature depend on the context of a study and may vary spatially and temporally. For example, the regulatory criterion for designating temperature-impaired streams in Oregon is based on the seven-day average of the daily maximum temperature, a timescale thought to be both reasonable for regulatory and management purposes and biologically relevant (Oregon Department of Environmental Quality, 2006a, 2006b). The value of this threshold metric varies both seasonally and spatially according to the designated biological use of a given river reach (for example, *rearing and migration* or *spawning*).

In this report, output from CE-QUAL-W2 was used to investigate the thermal regime at (1) daily and (2) monthly timescales, with some interannual comparison of monthly averages. A daily timescale (as the daily mean or daily maximum) is useful in assessing the spatial variation of stream temperature at a relatively short time scale and in assessing the acute thermal suitability of stream temperatures for aquatic species. Monthly averaged stream temperatures, in contrast, provide a better understanding of seasonal patterns and the chronic thermal exposure of aquatic species in the river system; monthly averages also tend to be more tractable for management actions. Finally, the comparison of monthly averages across multiple representative years provides insight into the "thermal template" of a river system, or the thermal conditions controlled by factors that change only over time scales of many years, such as climate, geomorphology, geology, and topography.

In addition to providing temporally discrete data that can be summarized at multiple timescales, output from spatially discrete models built with CE-QUAL-W2 also provide the opportunity to investigate spatial variations in stream temperature at multiple spatial scales. Temperature output for this report is provided at two scales: the segment scale, which provides a temperature for every segment in the model (ranging from about 100 to 500 m, depending on exact location in the modeling domain), and the "thermal-reach" scale, defined as river reaches of varying length with similar thermal patterns resulting from similar in-reach controls on temperature. Output at the segment scale is comparable to output from continuous monitoring stations in the main-stem river (which are placed to collect data representative of the main body of streamflow in the river, as opposed to micro-environments in off-channel or other features), but segment-scale results are available along the entire river network contained within the model domain as opposed to discrete monitoring locations. Analysis at the segment scale can be used to assess thermal conditions at specific locations in the river, to determine the spatial extent of temperatures within a certain threshold criterion, or to identify spatial variability in thermal minima and maxima at different time scales. In contrast, analysis at the thermal-reach scale can provide a better understanding of the thermal template of portions of the river system, their susceptibility to temperature manipulation from flow management, and a more synthesized assessment of the thermal suitability of river conditions for aquatic species.

Finally, stream temperature itself can be classified according to biologically relevant metrics. In this study, temperature was classified into four categories according to its probable effect on (1) juvenile Chinook salmon rearing and growth, and (2) adult Chinook salmon migration in the Willamette River (table 2; White and others, 2022). Based on an extensive literature review (for example, Brett, 1982; McCullough, 1999; Marine and Cech, Jr., 2004; Perry and others, 2015), this classification used the daily mean temperature as the best representation of conditions fish are exposed to over the course of a given day. Similar metrics for other life stages (for example, spawning and incubation) and for additional species of interest (for example, threatened winter-run steelhead) are beyond the scope of this study but may be investigated in future work.

In the following sections, output from CE-QUAL-W2 models of the Willamette River from its head (RM 187.2) to Willamette Falls (RM 26.8) was used to assess stream temperatures in the Willamette River using the metrics described above. This assessment was divided into two primary sections: first, an investigation of the baseline thermal template of the Willamette River upstream from Willamette Falls, which defined four characteristic thermal reaches (table 3) and assessed the stream temperature conditions for spring-run Chinook salmon, and second, an investigation into the sensitivity of stream temperature in the Willamette River upstream from Willamette Falls to flow-augmentation scenarios from four dams (via three tributaries to the Willamette River) and the potential effect of stream temperature management on spring-run Chinook salmon populations.

Table 3. Thermal-reach boundaries in the Willamette River upstream from Willamette Falls, Oregon, and continuous temperature monitors and streamflow gages within reach boundaries.

Included monitoring stations were active as of report publication (2022). [**Abbreviations**: RM, river mile; USGS, U.S. Geological Survey; USACE, U.S. Army Corps of Engineers]

Thermal reach	Upstream end of reach		Downstream end of reach		Thermal reach length (river miles)	Streamflow and temperature gages		
	Upstream end of reach	River mile	Downstream end of reach	River mile		Active streamflow gage or continuous temperature monitor	Data type	River mile
Springfield-McKenzie Reach	Confluence of Middle Fork Willamette and Coast Fork Willamette Rivers, near Springfield	187.2	McKenzie River confluence	175.5	11.7	USACE EUGO3, Willamette River at Eugene	Streamflow	182.5
						USGS 14158100, Willamette River at Owosso Bridge at Eugene (RM 178.8)	Temperature	178.8
McKenzie-Santiam Reach	McKenzie River confluence	175.5	Santiam River confluence	109.0	66.5	USGS 14166000, Willamette River at Harrisburg	Streamflow, temperature	161.0
						USGS 14171600, Willamette River at Corvallis	Streamflow	131.4
						USGS 14174000, Willamette River at Albany	Streamflow, temperature	119.3
Santiam-Newberg Reach	Santiam River confluence	109.0	Head of Newberg Pool	50.0	59.0	USGS 14191000, Willamette River at Salem	Streamflow	84.2
						USGS 14192015, Willamette River at Keizer	Temperature	82.2
Newberg Pool Reach	Head of Newberg Pool	50.0	Willamette Falls	26.8	23.2	USGS 14197900, Willamette River at Newberg	Streamflow, temperature	50.0

Willamette River Thermal Template

Model results for Willamette River water temperatures on daily and monthly timescales during 2011, 2015, and 2016 showed similar seasonal and longitudinal patterns but a wide range of annual variability across the thermal landscape (figs. 3*A*–*C*). In a general sense, the Willamette River was cool in spring, warmed downstream and through the summer, then cooled in autumn. In 2015, the Willamette River from its head to Willamette Falls warmed from a monthly mean water temperature of 12.0 °C in April to 22.1 °C in July, with monthly mean water temperatures above 20 °C in June, July, and August (table 4). June air temperatures in 2015 were abnormally high, and the maximum daily water temperature in 2015 was modeled to occur in a model segment immediately upstream from Newberg, reaching 27.5 °C in early July (fig. 2; table 5). In 2016, as modeled, the river warmed more slowly, with a monthly mean water temperature of 17.7 °C in June and mean monthly temperature above 20 °C only in July and August (table 4). Heating in the Willamette River during 2016 was not as extreme as in 2015, with the daily maximum water temperature peaking at 25.7 °C in July of 2016, also immediately upstream from Newberg (table 5). While hydroclimatological conditions in 2016 were less extreme than in 2015, the models revealed that the mean temperature of the Willamette River in 2016 during the study season was only 1.2 °C cooler. In contrast, the 2011 study season was an average of 3.6 °C cooler than in 2015 and 2.4 °C cooler than in 2016 (table 4). Peak water temperatures in 2011 occurred in early and late August, with an annual daily maximum of 22.8 °C from Keizer to Willamette Falls (table 5). The monthly mean water temperature in June of 2011 was only 13.8 °C, and no months exceeded 20 °C with the highest monthly mean water temperature of 18.5 °C in August (table 4).

To allow comparison of interannual variability in stream temperature, modeled temperatures in 2011, 2015, and 2016 were plotted as a monthly averaged longitudinal profile. The monthly scale removes the visible influence of transient hydroclimatological conditions like storms or heat waves, allowing a better interannual comparison and the investigation of the thermal template of the Willamette River and its longitudinal variability. Although monthly averaged temperatures varied among years, the longitudinal rates of temperature change were similar (fig. 4). As modeled in 2011, 2015, and 2016, the Willamette River was cool in April (from 8 °C to about 11 °C at its head, depending on year) and downstream warming was limited, with a monthly averaged temperature difference from the head of the Willamette River to Willamette Falls of several degrees Celsius or less. As seasonal heat loads increased into the summer, the downstream reaches of the Willamette River warmed more than the upstream reaches to the model, creating a steeper temperature gradient from the head of the Willamette River to Willamette Falls during summer months when compared to April. Annual stream temperatures in the Willamette River peaked in late July or early August, then began to cool in late summer (fig. 3; table 5). By October, seasonal cooling was greater in the lower reaches of the Willamette River than along the upper river corridor, creating a relatively isothermal (within about 1 degree Celsius) longitudinal temperature profile, except for the uppermost section of the Willamette River upstream from the McKenzie River confluence. Heat accumulated within Lookout Point and Dexter Lakes during the summer and exported downstream from Lookout Point and Dexter Dams to the Middle Fork Willamette River in autumn caused the Willamette River to be warmer upstream from the McKenzie River confluence than in the rest of the Willamette River (fig. 4).

Discontinuities in the thermal profile of the Willamette River caused by tributary confluences were evident at both daily and monthly timescales (figs. 3, 4). Both the McKenzie and Santiam Rivers caused thermal discontinuities in the Willamette River that persisted across all modeled seasons, whereas smaller tributaries like the Long Tom, Calapooia, or Yamhill Rivers had both a smaller and more transient effect on the temperature of the Willamette River. For example, the Willamette River was warmer downstream from the Yamhill River confluence in April of 2011 (when streamflow from the relatively warmer Yamhill River was high), but this effect was not evident in the summer or autumn (fig. 4). The effect of tributaries on Willamette River temperatures can be greater than 2 °C during certain times of year but is typically less. For example, the McKenzie River tended to change the temperature of the Willamette River by about 1 °C in August. The temperature effect of the Santiam River tended to be on the order of tenths to half of a degree Celsius for most of the year but as much as 1.5 °C in late summer (figs. 3, 4). The effect of smaller, unregulated tributaries like the Calapooia or Yamhill Rivers may have had a small effect on temperatures in the Willamette River on a daily basis, particularly in spring when their streamflows are higher, but any effects of these small tributaries were nearly negligible at the monthly scale.

At the monthly averaged scale, temperatures and the longitudinal rate of temperature change in the Newberg Pool were not notably different from the river reach downstream from the Santiam River confluence. However, daily plots show that the Newberg Pool was distinct from the reaches upstream in the timing of its thermal response to heat loading. The pattern of vertical striping visible in figure 3 upstream from Newberg indicated the Willamette River responds to river-scale changes in heat fluxes (weather) approximately synchronously; in other words, the hottest days or weeks of the year tended to occur on the same day along all reaches of the river. In the Newberg Pool downstream from RM 50, however, peak temperatures occurred on progressively later days with distance downstream, producing a “lagged” temperature pattern in the Newberg Pool relative to the non-pooled reaches upstream (as shown by the “bend” to the right visible in thermal patterns starting near RM 50; fig. 3).

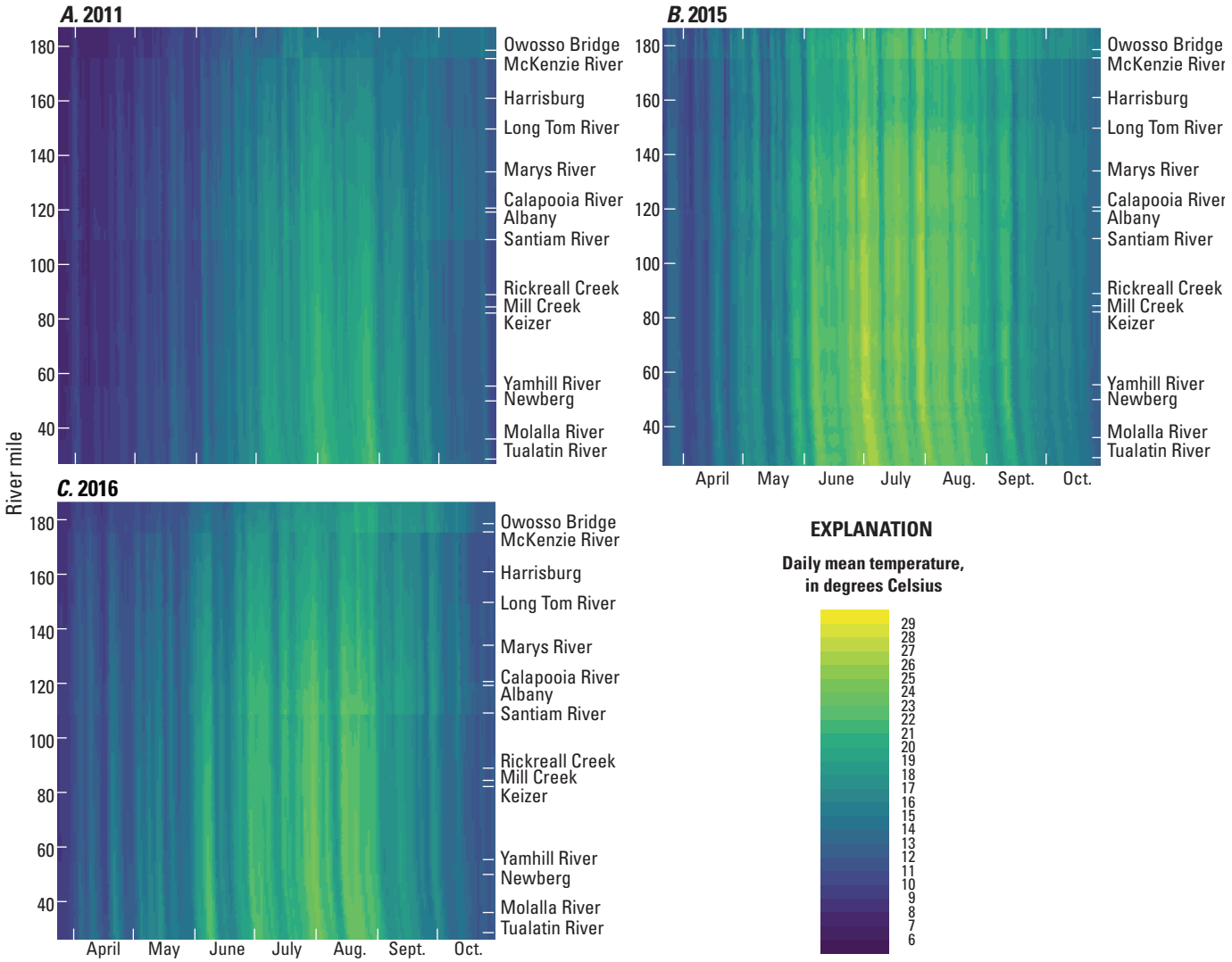

Figure 3. Modeled baseline daily mean temperatures in the Willamette River from its head at the confluence of the Coast Fork Willamette and Middle Fork Willamette Rivers at river mile 187.2 to Willamette Falls at river mile 26.8 during March 24 (*A*, *B*) or March 23 (*C*) through October 30 (2011, 2015) or October 29 (2016), northwestern Oregon. Streams annotated on y-axis are those included as tributaries in the model; other annotated locations are U.S. Geological Survey continuous temperature monitoring stations, including: 14158100, Willamette River at Owosso Bridge at Eugene; 14166000, Willamette River at Harrisburg; 14174000, Willamette River at Albany; 14192015, Willamette River at Keizer; and 14197900, Willamette River at Newberg (U.S. Geological Survey, 2020).

Table 4. Modeled monthly mean (reach-averaged daily mean water temperature), in degrees Celsius, of baseline modeled conditions in the Willamette River, northwestern Oregon, in 2011, 2015, and 2016.

[See text for definition of reach boundaries. Willamette River reach includes the entire modeled domain from the head of the river at the confluence of the Coast Fork Willamette and Middle Fork Willamette Rivers near Springfield to Willamette Falls]

Reach	Monthly mean water temperature, in degrees Celsius							
	April	May	June	July	August	September	October	Season Average
				2011				
Springfield-McKenzie	8.1	9.6	12.1	14.8	15.0	14.8	14.5	12.7
McKenzie-Santiam	8.9	10.7	13.5	16.9	17.5	15.3	13.2	13.7
Santiam-Newberg	9.1	11.0	14.2	18.4	19.6	16.3	12.7	14.5
Newberg Pool	9.4	11.6	14.7	18.8	20.6	17.1	12.8	15.0
Willamette River	9.0	10.9	13.8	17.6	18.5	15.9	13.0	14.1
				2015				
Springfield-McKenzie	11.4	13.7	17.2	19.5	19.4	17.7	15.6	16.4
McKenzie-Santiam	11.8	15.1	19.4	21.3	20.4	17.2	14.5	17.2
Santiam-Newberg	12.2	16.1	21.1	23.0	21.8	17.6	14.7	18.1
Newberg Pool	12.6	16.4	21.6	23.5	22.5	18.0	14.8	18.5
Willamette River	12.0	15.6	20.2	22.1	21.2	17.5	14.7	17.7
				2016				
Springfield-McKenzie	10.4	11.7	14.7	17.5	19.0	17.6	14.4	15.1
McKenzie-Santiam	11.8	13.4	17.0	19.5	19.9	17.1	13.2	16.0
Santiam-Newberg	12.5	14.6	18.5	21.1	21.5	17.2	13.1	17.0
Newberg Pool	13.1	15.1	18.9	21.3	22.1	17.5	13.4	17.4
Willamette River	12.1	14.0	17.7	20.2	20.8	17.2	13.3	16.5

Table 5. Modeled daily maximum water temperature by month and reach, in degrees Celsius, of baseline conditions in the Willamette River, northwestern Oregon, in 2011, 2015, and 2016.

[See text for definition of reach boundaries. Willamette River reach includes the entire modeled domain from the head of the river at the confluence of the Coast Fork Willamette and Middle Fork Willamette Rivers near Springfield to Willamette Falls.]

Reach	Daily maximum water temperature, in degrees Celsius							
	April	May	June	July	August	September	October	Season Maximum
				2011				
Springfield-McKenzie	10.7	13.0	16.6	19.8	18.3	17.3	15.9	19.8
McKenzie-Santiam	11.7	14.1	18.1	21.6	21.4	18.5	16.2	21.6
Santiam-Newberg	11.7	14.1	18.0	22.3	22.8	19.9	16.0	22.8
Newberg Pool	11.4	13.9	17.8	22.2	22.8	20.3	15.0	22.8
Willamette River	11.7	14.1	18.1	22.3	22.8	20.3	16.2	22.8
				2015				
Springfield-McKenzie	16.4	19.1	22.8	24.4	23.3	21.5	17.8	24.4
McKenzie-Santiam	16.2	20.7	25.0	26.5	26.5	21.7	16.9	26.5
Santiam-Newberg	16.3	21.5	25.3	27.5	27.0	22.6	17.1	27.5
Newberg Pool	16.3	21.5	25.3	27.1	26.4	22.2	16.6	27.1
Willamette River	16.4	21.5	25.3	27.5	27.0	22.6	17.8	27.5
				2016				
Springfield-McKenzie	13.4	16.1	20.3	21.9	23.5	20.5	18.0	23.5
McKenzie-Santiam	15.3	18.2	23.4	24.6	24.3	20.8	17.6	24.6
Santiam-Newberg	16.7	18.1	23.2	25.7	25.0	21.0	17.5	25.7
Newberg Pool	17.0	18.0	23.3	25.6	25.1	22.0	17.6	25.6
Willamette River	17.0	18.2	23.4	25.7	25.1	22.0	18.0	25.7

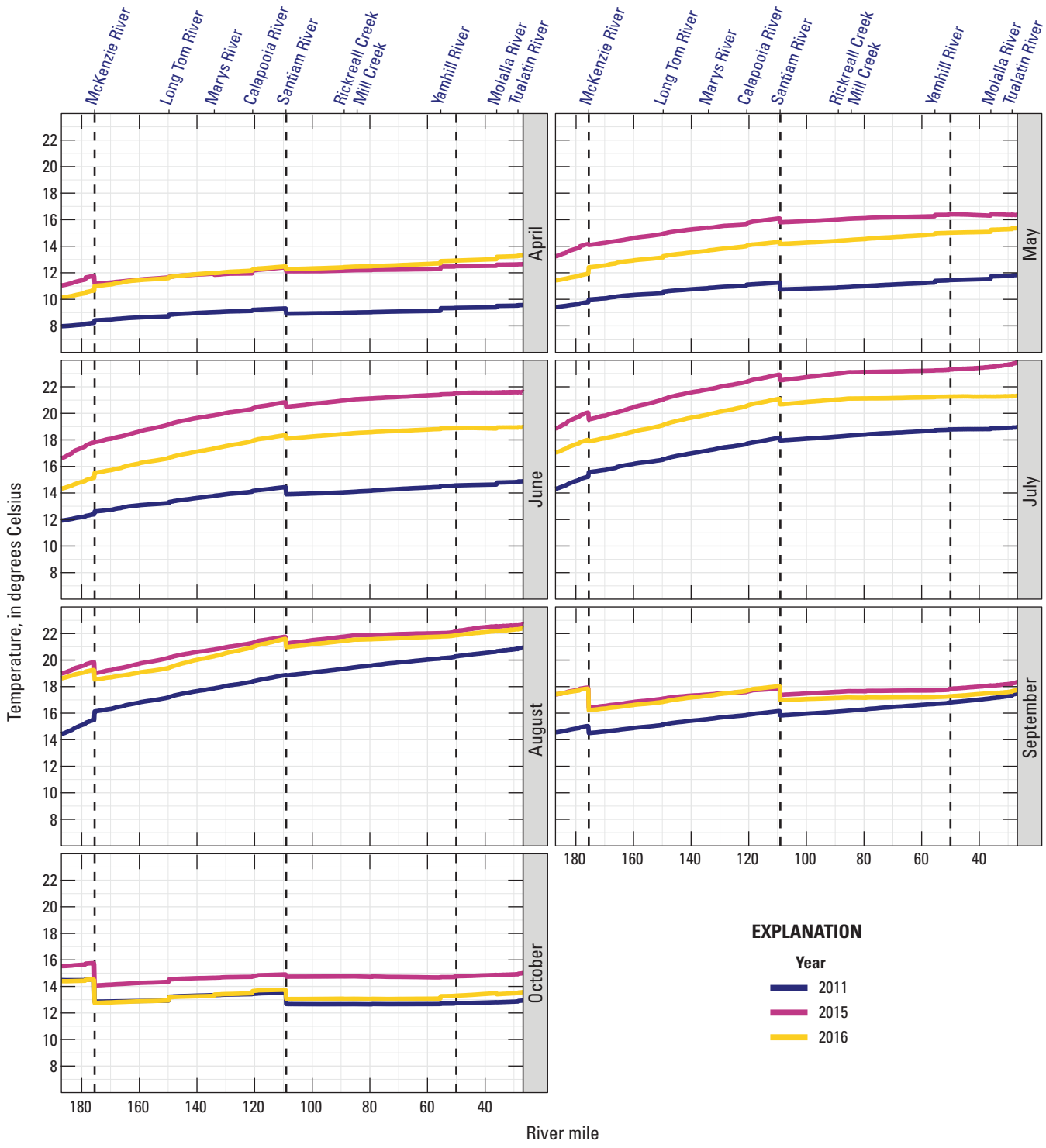

Figure 4. Monthly mean longitudinal profile of the daily mean modeled water temperature along the Willamette River, northwestern Oregon, for 2011, 2015, and 2016, in degrees Celsius. Streams annotated on x-axis are those included as tributaries in the model. Dashed vertical lines separate designated thermal reaches, from upstream to downstream: (1) Springfield-McKenzie Reach, (2) McKenzie-Santiam Reach, (3) Santiam-Newberg Reach, and (4) Newberg Pool.

Combining the observation of tributary-derived thermal discontinuities, differences in the longitudinal rates of temperature change, and lags in temperature response, the Willamette River can be divided into four characteristic "thermal reaches":

- **Springfield-McKenzie Reach:** The Springfield-McKenzie Reach is 11.7 miles long, from the head of the Willamette River at RM 187.2 to the McKenzie River confluence at RM 175.5. For most of the year during the 3 years modeled, the Springfield-McKenzie Reach was the coolest part of the river but had the largest rate of downstream warming. In contrast, in late summer and early autumn when the river started to cool from its mid-summer maximum, the Springfield-McKenzie Reach was the warmest part of the river (fig 4). One continuous temperature monitor is located in this reach: USGS 14158100 (Willamette River at Owosso Bridge at Eugene (RM 178.8).

- **McKenzie-Santiam Reach:** The McKenzie-Santiam Reach is 66.5 miles long, from the McKenzie River confluence to the Santiam River confluence at RM 109.0. The McKenzie-Santiam Reach is strongly influenced by the McKenzie River, but the effect varies by year and season. In 2011, the McKenzie River warmed the Willamette River from April until August and cooled it in September and October (fig. 4). This pattern was repeated in 2016, except that the McKenzie River had a net cooling effect on the Willamette River earlier in the year, in July. In 2015, the effect of the McKenzie River was smaller but was always to cool the Willamette River. The downstream, monthly averaged warming rate in the McKenzie-Santiam Reach is the second steepest of the four reaches. The lower miles of the McKenzie-Santiam Reach, from approximately Albany to the Santiam River confluence, have nearly the same cumulative degree-day heating (the sum of mean daily temperature exposure above 0 °C) in July and August as the lower reaches of the Santiam-Newberg Reach downstream (fig. 5). Continuous temperature monitors within this reach include USGS 14166000, Willamette River at Harrisburg (RM 161.0) and USGS 14174000, Willamette River at Albany (RM 119.3).

- **Santiam-Newberg Reach:** The Santiam-Newberg Reach is 59 miles long, from the confluence of the Santiam River to the start of the Newberg Pool at RM 50.0. Like the McKenzie-Santiam Reach, it is strongly influenced by the tributary demarking its upper boundary. The net effect of the Santiam River on the Santiam-Newberg Reach, however, is both smaller and more consistent than the McKenzie River. With the exception of August 2011, the Santiam River consistently cooled the Willamette River in all modeled time periods. Except for the Newberg Pool, the Santiam-Newberg Reach has the lowest rate of downstream warming among the four defined reaches (fig. 4). On a daily basis, the lower miles of the Santiam-Newberg Reach, upstream from the Newberg Pool, may have the hottest temperatures (warmest daily maxima) in the Willamette River upstream from Willamette Falls (fig. 3). Continuous temperature monitors in this reach include USGS 14192015, Willamette River at Keizer (RM 84.2) and USGS 14197900, Willamette River at Newberg (RM 50.0).

- **Newberg Pool Reach:** The Newberg Pool Reach is 23.2 miles long, from Newberg to Willamette Falls at RM 26.8. Averaged over July and August, the Newberg Pool has the greatest total heat load in the Willamette River (fig. 5) but daily maximum temperatures in the Newberg Pool may be slightly cooler than daily maxima in portions of the Santiam-Newberg Reach upstream, depending on the rate of response to thermal inputs. Major tributaries entering the Newberg Pool include the Molalla and Tualatin Rivers, but model results show that these rivers have only a small influence on the temperature of the Willamette River. One temperature sensor, USGS 14197000, Willamette River at Newberg, is located at the head of the Newberg Pool but is generally more indicative of conditions at the downstream end of the Santiam-Newberg Reach.

Many of the characteristics of these four reaches can be illustrated by computing the difference of the daily mean temperature of each segment and the daily mean temperature at RM 50.0, the head of the Newberg Pool (fig. 6). Across all modeled years, the maximum downstream warming from the head of the Willamette River to the head of the Newberg pool was within several tenths of 7.5 °C; the maximum downstream cooling is within several tenths of 3.5 °C. The multi-day travel time through the Newberg Pool and its large heat content caused the computed temperature difference to be alternately cooler and warmer than at the head of the Newberg Pool as upstream reaches heated or cooled more quickly in response to the weather. The rate and amount of downstream warming or cooling was interrupted by the McKenzie and Santiam Rivers, but in general the river upstream from the Newberg Pool warmed downstream in the spring and summer but had a variable heating or cooling profile in autumn.

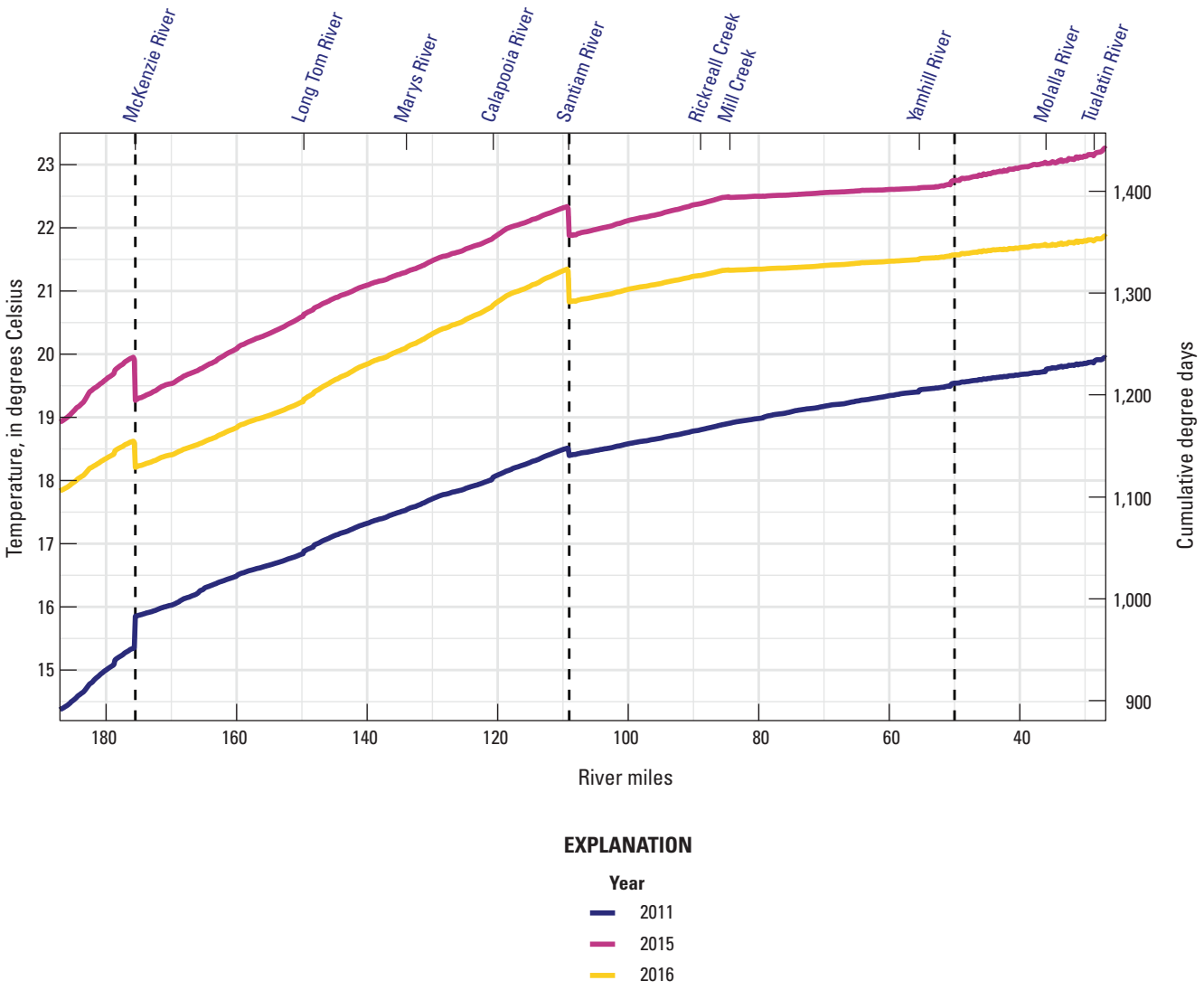

Figure 5. Longitudinal profiles of modeled mean water temperature and cumulative degree days (the sum of mean daily temperature exposure above 0 degrees Celsius) for July and August 2011, 2015, and 2016, Willamette River, northwestern Oregon. Streams annotated on x-axis are those included as tributaries in the model. Dashed vertical lines separate designated thermal reaches, from upstream to downstream: (1) Springfield-McKenzie Reach, (2) McKenzie-Santiam Reach, (3) Santiam-Newberg Reach, and (4) Newberg Pool.

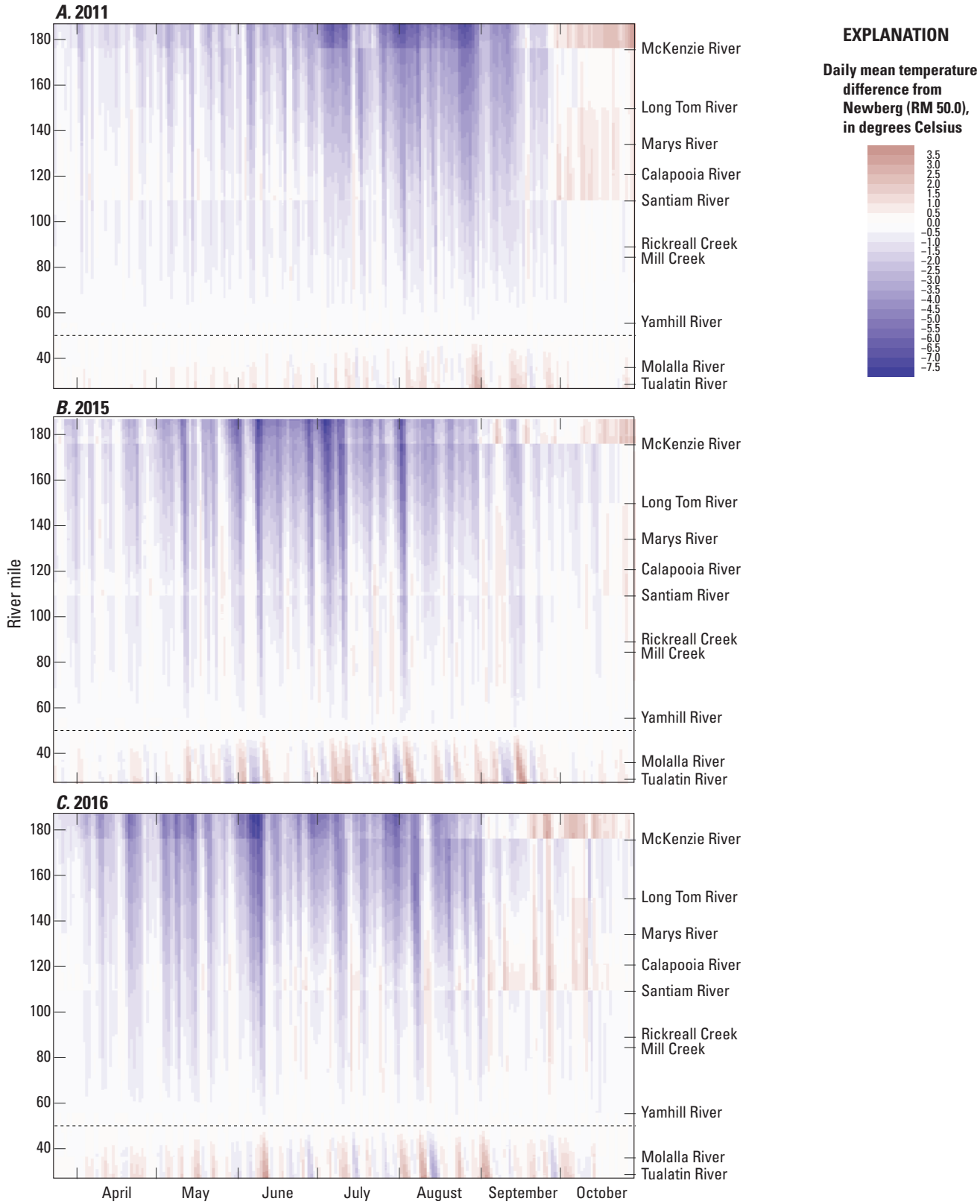

Figure 6. Difference in modeled daily mean temperatures in (*A*) 2011, (*B*) 2015, and (*C*) 2016, relative to the modeled daily mean water temperature at river mile 50.0 (Newberg), Willamette River, northwestern Oregon. Streams annotated on y-axis are those included as tributaries in the model.

Temperature Conditions for Spring-Run Chinook Salmon

To better understand the influence of thermal conditions in the Willamette River on threatened cold-water fish populations, temperatures in the river were classified into categories defined by their effects on different life stages of Chinook salmon (table 2; White and others, 2022). In all three modeled years, conditions were favorable (classified as optimal or suboptimal, which may limit growth rates) for juvenile and adult Chinook salmon during most of spring and autumn (figs. 7, 8). In 2015 and 2016, optimal conditions extended across the entire Willamette River through May and parts of June; in 2011, optimal conditions for juvenile Chinook salmon extended through most of July. In all years, optimal conditions for juveniles and adults returned to the Willamette River beginning in September. In 2011, two periods during late July–early August and late August were marked by adversely warm conditions for juveniles (≥ 20 °C), extending upstream more than 90 river miles as far as approximately RM 120, near Albany. For most of May through October of 2011 along the entire modeled river length, however, the majority of the Willamette River was classified as optimal for juvenile Chinook salmon.

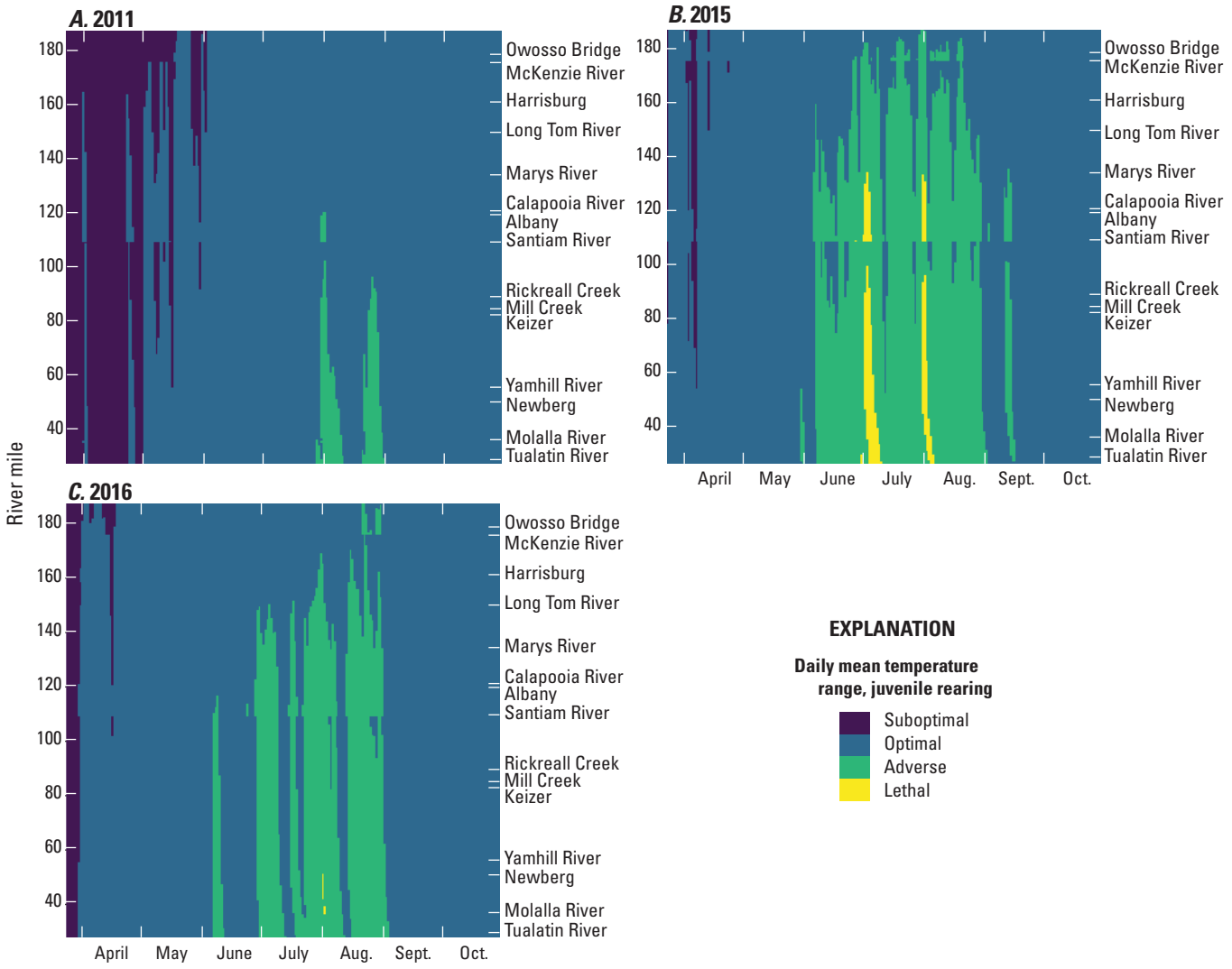

Figure 7. Modeled temperature category for juvenile Chinook salmon (*Oncorhynchus tshawytscha*) rearing and growth in (*A*) 2011, (*B*) 2015, and (*C*) 2016, Willamette River, northwestern Oregon. Temperature ranges for the categories are defined in table 2. Streams annotated on y-axis are those included as tributaries in the model; other annotated locations are U.S. Geological Survey continuous temperature monitoring stations, including: 14158100, Willamette River at Owosso Bridge at Eugene; 14166000, Willamette River at Harrisburg; 14174000, Willamette River at Albany; 14192015, Willamette River at Keizer; and 14197900, Willamette River at Newberg (U.S. Geological Survey, 2020).

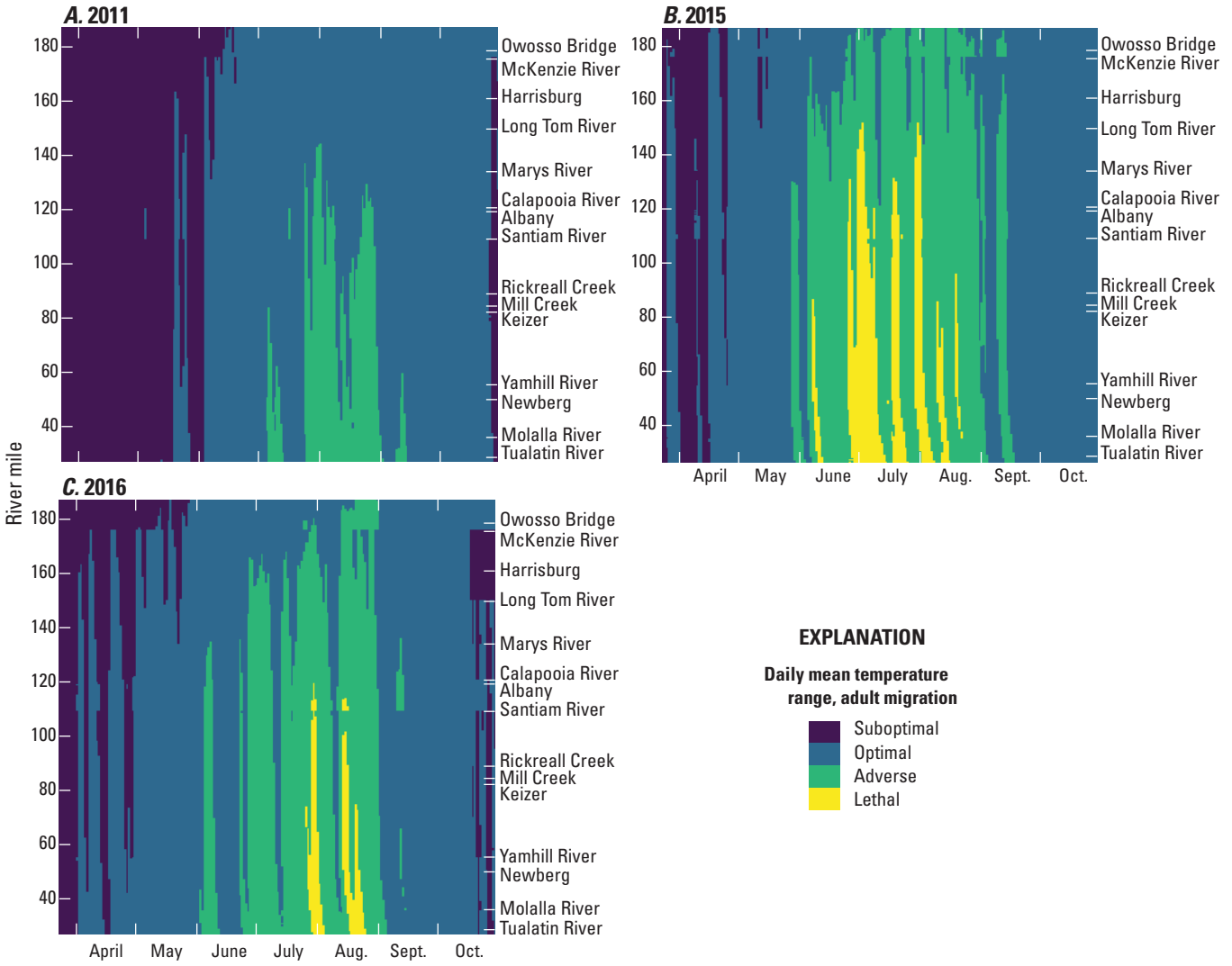

Figure 8. Modeled temperature category for adult Chinook salmon (*Oncorhynchus tshawytscha*) migration in (*A*) 2011, (*B*) 2015, and (*C*) 2016, Willamette River, northwestern Oregon. Temperature ranges for the categories are defined in table 2. Streams annotated on y-axis are those included as tributaries in the model; other annotated locations are U.S. Geological Survey continuous temperature monitoring stations, including: 14158100, Willamette River at Owosso Bridge at Eugene, Willamette River at Harrisburg; 14174000, Willamette River at Albany; 14192015, Willamette River at Keizer; and 14197900, Willamette River at Newberg (U.S. Geological Survey, 2020).

In the summers of 2015 and 2016, Willamette River thermal conditions were more unfavorable for both juvenile and adult Chinook salmon. With a few cooler periods interspersed, adversely warm stream temperatures were pervasive through July, August, and parts of June in 2016, often extending as far upstream as the Marys River confluence (RM 134.0), and for several days as far upstream as the head of the Willamette River at RM 187.2 (the upstream limit of the model domain; figs. 7, 8). Conditions in 2015 were more extreme than in 2016, with adverse conditions common as far upstream as Harrisburg (RM 160, approximately 133 miles from Willamette Falls) or farther. Additionally, as modeled, the Willamette River upstream from Willamette Falls was categorized as lethally warm for both juvenile and adult Chinook salmon for periods of the summers of 2015 and 2016 approximately as far upstream as the Marys River confluence (RM 134.0) and the Rickreall Creek confluence (RM 89.0), respectively. Summarized for July of 2015, 17 percent of the modeled river length upstream from Willamette Falls could be classified as lethal for juveniles (table 6; fig. 7). During two periods in July and August of 2015, lethal conditions for juveniles are modeled to have extended as far upstream as approximately the Marys River confluence at RM 134.0. For adults, which have a more restricted thermal tolerance, lethal conditions occurred both more frequently and with greater extent (fig. 8). During July of 2015, 33 percent of the modeled river length upstream from Willamette Falls could be classified as lethal for adults (table 7). At times, lethal conditions extended as far upstream as the Long Tom River confluence at RM 149.7 (nearly 123 miles from Willamette Falls; fig 8*B*).

Table 6. Length of the Willamette River (head to Willamette Falls), northwestern Oregon, within designated temperature range for juvenile Chinook salmon (*Oncorhynchus tshawytscha*) rearing and growth grouped by month, as percentage.

[See table 2 for definition of temperature ranges for the thermal categories.]

Thermal category	Percentage of river length						
	April	May	June	July	August	September	October
				2011			
Lethal	0	0	0	0	0	0	0
Adverse	0	0	0	7	23	0	0
Optimal	13	79	99	93	77	100	100
Suboptimal	88	21	1	0	0	0	0
				2015			
Lethal	0	0	2	17	4	0	0
Adverse	0	3	59	69	74	8	0
Optimal	92	97	39	14	22	92	100
Suboptimal	8	0	0	0	0	0	0
				2016			
Lethal	0	0	0	2	1	0	0
Adverse	0	0	17	56	67	1	0
Optimal	97	100	83	42	32	99	100
Suboptimal	3	0	0	0	0	0	0

Table 7. Length of Willamette River (head to Willamette Falls) in northwestern Oregon within designated temperature range for adult Chinook salmon (*Oncorhynchus tshawytscha*) migration grouped by month, as percentage.

[See table 2 for definition of temperature ranges for the thermal categories.]

Thermal category	Percentage of river length						
	April	May	June	July	August	September	October
				2011			
Lethal	0	0	0	0	0	0	0
Adverse	0	0	0	20	44	2	0
Optimal	0	14	85	80	56	98	87
Suboptimal	100	86	15	0	0	0	13
				2015			
Lethal	0	0	9	33	11	0	0
Adverse	0	6	63	62	81	20	0
Optimal	45	93	27	5	8	80	100
Suboptimal	55	1	0	0	0	0	0
				2016			
Lethal	0	0	0	6	9	0	0
Adverse	0	0	28	67	72	4	0
Optimal	49	90	72	26	19	96	79
Suboptimal	51	10	0	0	0	0	21

Table 8. Range of difference in daily mean and daily maximum temperatures for uniform flow augmentation of 1,000 cubic feet per second over baseline conditions from Dexter (Middle Fork Willamette River), Cougar (South Fork McKenzie River), Foster (South Santiam River), or Big Cliff (North Santiam River) Dams compared to modeled baseline conditions in 2011, 2015, and 2016, Willamette River, northwestern Oregon.

Source of flow augmentation	Daily mean temperature		Daily maximum temperature	
	Maximum cooling (degrees Celsius)	Maximum warming (degrees Celsius)	Maximum cooling (degrees Celsius)	Maximum warming (degrees Celsius)
2011				
Dexter Dam (Middle Fork Willamette River)	-0.8	0.2	-1.3	0.3
Cougar Dam (South Fork McKenzie River)	-0.6	0.5	-1.1	1.2
Foster Dam (South Santiam River)	-0.8	0.1	-1.3	0.3
Big Cliff Dam (North Santiam River)	-0.7	0.0	-0.8	0.1
2015				
Dexter Dam (Middle Fork Willamette River)	-1.0	0.8	-1.4	0.9
Cougar Dam (South Fork McKenzie River)	-1.1	0.4	-1.4	0.7
Foster Dam (South Santiam River)	-1.4	0.2	-1.7	0.3
Big Cliff Dam (North Santiam River)	-1.4	0.3	-1.7	0.4
2016				
Dexter Dam (Middle Fork Willamette River)	-0.7	0.9	-1.1	0.9
Cougar Dam (South Fork McKenzie River)	-1.0	0.5	-1.4	0.8
Foster Dam (South Santiam River)	-1.1	0.3	-1.6	0.5
Big Cliff Dam (North Santiam River)	-1.2	0.3	-1.7	0.5

Influence of Flow Augmentation

To better understand the influence of flow management on stream temperature in the Willamette River, flow-augmentation scenarios were modeled for each of the three model years. One thousand cubic feet per second of additional flow was uniformly added to the baseline dam releases into the Coast Fork Willamette and Middle Fork Willamette River submodel (from Dexter Dam on the Middle Fork Willamette River; 16.5 miles upstream from the head of the Willamette River at RM 187.2), McKenzie River submodel (from Cougar Dam on the South Fork McKenzie River; approximately 60.6 miles upstream from the McKenzie River-Willamette River confluence), South Santiam River submodel (from Foster Dam on the South Santiam River, approximately 48.3 miles upstream from the Santiam-Willamette River confluence), or North Santiam and Santiam River submodels (from Big Cliff Dam on the North Santiam River, approximately 58.6 miles upstream from the Santiam-Willamette River confluence). These flow-augmentation scenarios simulated additional flow from storage in Lookout Point/Dexter Lakes, Cougar Reservoir, Green Peter/Foster Lakes, or Detroit/Big Cliff Lakes, respectively. Results from these scenarios showed that the effects of flow augmentation on temperatures in the Willamette River was not uniform. The magnitude and even direction (cooling versus warming) of influence on stream temperature in the Willamette River varied by source, location, pre-existing river and lake conditions, and season.

Across all modeled scenarios in all years, the effect of flow augmentation ranged from -1.4 to 0.9 °C on the daily mean stream temperature and -1.7 to 1.2 °C on the daily maximum stream temperature in any individual modeled segment of the Willamette River (table 8). The largest cooling or warming effects were limited in extent and duration to a few days at a few locations (figs. 9–11); however, some cooling often was predicted to occur at the times and locations when conditions were detrimental to cold-water fishes, generally in mid-summer and in the more-downstream river reaches. In general, the range of influence was limited to 1 °C or (much) less, depending on location in the Willamette River and the source of the additional streamflow. On a monthly, reach-averaged basis, the effect of flow augmentation on daily mean temperature ranged from negligible (< ±0.1 °C) to a maximum cooling effect of -0.5 °C in 2011 and -0.9 °C in 2015 and 2016 and a maximum *warming* effect of 0.1 °C in the Santiam-Newberg Reach in 2011 and 0.5 °C in the Springfield-McKenzie Reach and Santiam-Newberg Reaches in 2015 and 0.5 °C in the Springfield-McKenzie Reach in 2016 (table 9). Averaged over all reaches and across the modeling period from April to October, the scale of effect ranged from -0.1 °C in 2011 to -0.3 °C in 2015.

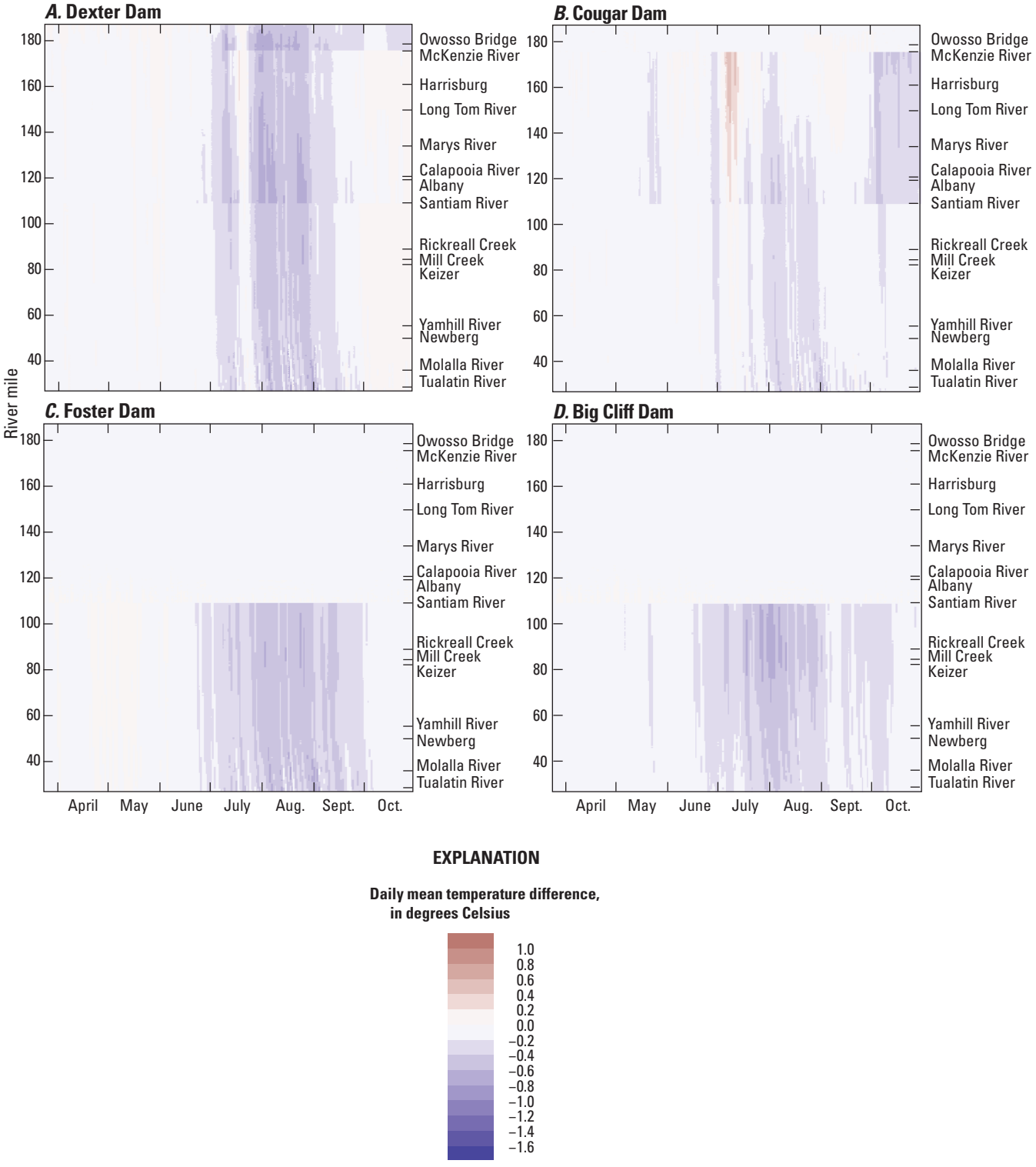

Figure 9. Difference from 2011 baseline conditions in modeled daily mean temperature in the Willamette River from its head at the confluence of the Coast Fork Willamette and Middle Fork Willamette Rivers at river mile (RM) 187.2 to Willamette Falls at RM 26.8 with additional flow of 1,000 cubic feet per second above baseline from (*A*) Dexter Dam on the Middle Fork Willamette River, (*B*) Cougar Dam on the South Fork McKenzie River, (*C*) Foster Dam on the South Santiam River, and (*D*) Big Cliff Dam on the North Santiam River, northwestern Oregon. Streams annotated on y-axis are those included as tributaries in the model; other annotated locations are U.S. Geological Survey (2020) continuous temperature monitoring stations, including: 14158100, Willamette River at Owosso Bridge at Eugene; 14166000, Willamette River at Harrisburg; 14174000, Willamette River at Albany; 14192015, Willamette River at Keizer; and 14197900, Willamette River at Newberg.

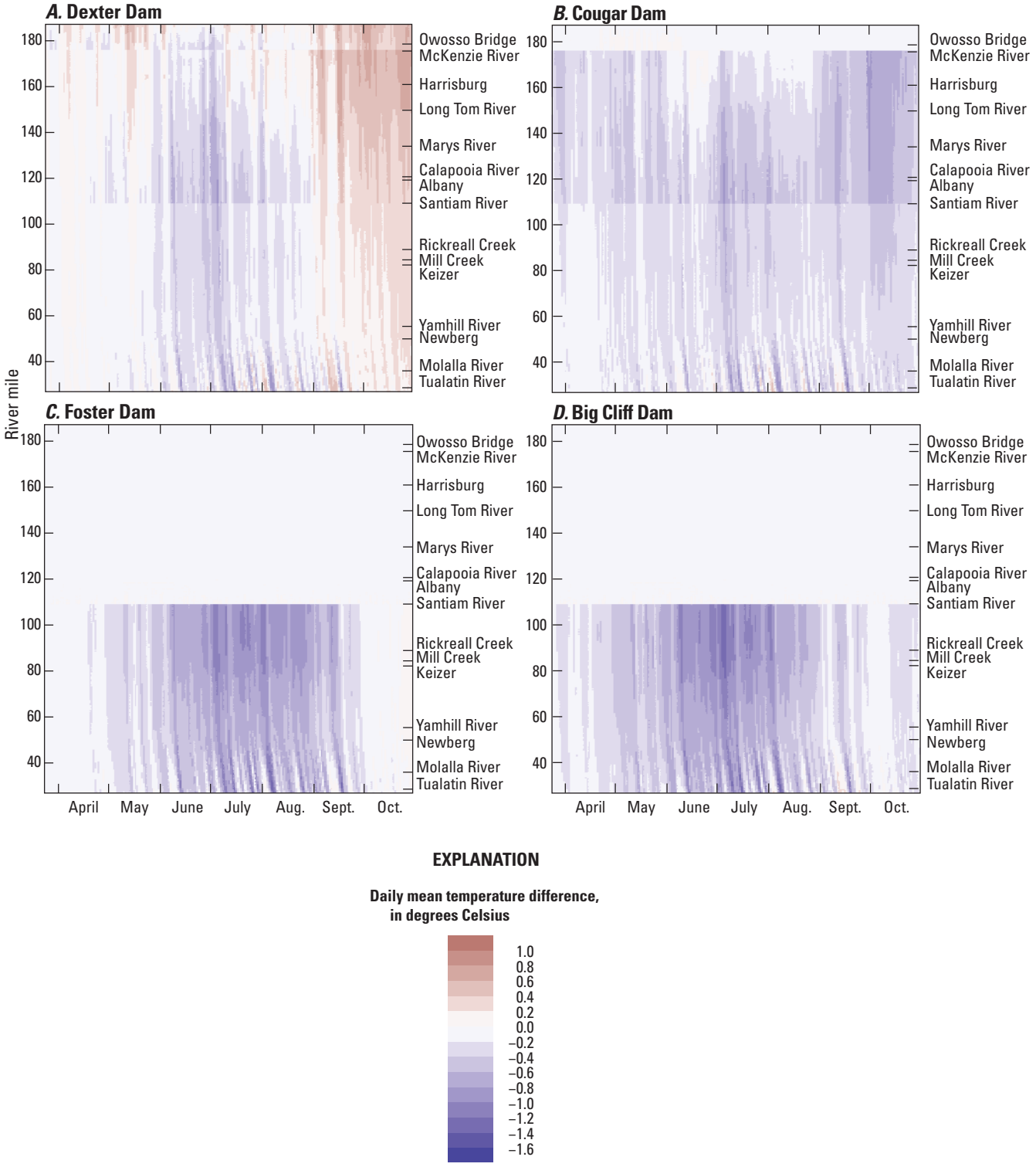

Figure 10. Difference from 2015 baseline conditions in modeled daily mean temperature in the Willamette River from its head at the confluence of the Coast Fork Willamette and Middle Fork Willamette Rivers at river mile (RM) 187.2 to Willamette Falls at RM 26.8 with additional flow of 1,000 cubic feet per second above baseline from (*A*) Dexter Dam on the Middle Fork Willamette River, (*B*) Cougar Dam on the South Fork McKenzie River, (*C*) Foster Dam on the South Santiam River, and (*D*) Big Cliff Dam on the North Santiam River, northwestern Oregon. Streams annotated on y-axis are those included as tributaries in the model; other annotated locations are U.S. Geological Survey (2020) continuous temperature monitoring stations, including: 14158100, Willamette River at Owosso Bridge at Eugene; 14166000, Willamette River at Harrisburg; 14174000, Willamette River at Albany; 14192015, Willamette River at Keizer; and 14197900, Willamette River at Newberg.

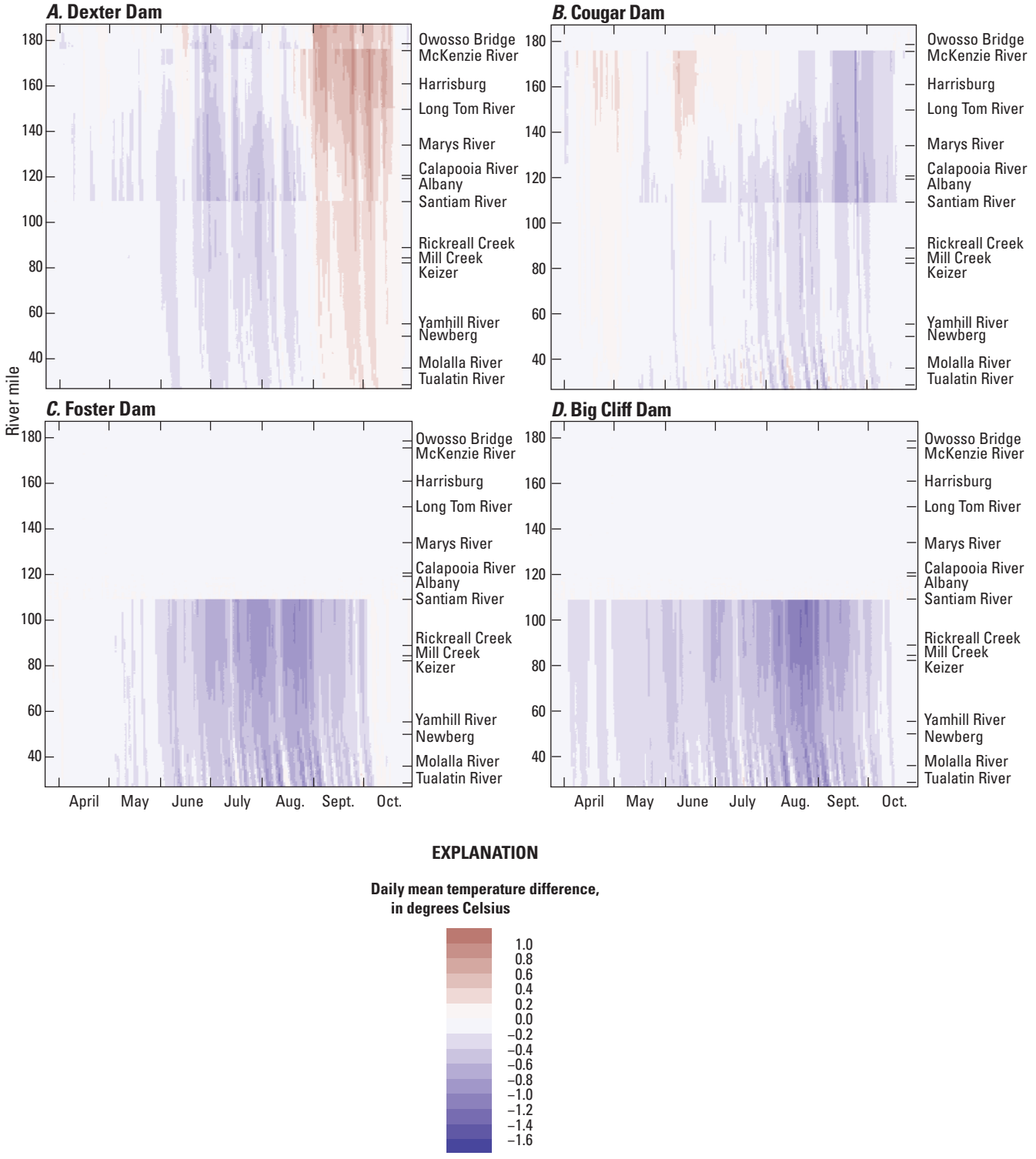

Figure 11. Difference from 2016 baseline conditions in modeled daily mean temperature in the Willamette River from its head at the confluence of the Coast Fork Willamette and Middle Fork Willamette Rivers at river mile (RM) 187.2 to Willamette Falls at RM 26.8 with additional flow of 1,000 cubic feet per second above baseline from (*A*) Dexter Dam on the Middle Fork Willamette River, (B) Cougar Dam on the South Fork McKenzie River, (*C*) Foster Dam on the South Santiam River, and (*D*) Big Cliff Dam on the North Santiam River, northwestern Oregon. Streams annotated on y-axis are those included as tributaries in the model; other annotated locations are U.S. Geological Survey (2020) continuous temperature monitoring stations, including: 14158100, Willamette River at Owosso Bridge at Eugene; 14166000, Willamette River at Harrisburg; 14174000, Willamette River at Albany; 14192015, Willamette River at Keizer; and 14197900, Willamette River at Newberg.

Table 9. Monthly averaged difference in daily mean temperatures, by thermal reach, for uniform flow augmentation of 1,000 cubic feet per second over baseline conditions from Dexter (Middle Fork Willamette River), Cougar (South Fork McKenzie River), Foster (South Santiam River), or Big Cliff (North Santiam River) Dams, northwestern Oregon, compared to modeled baseline conditions in 2011, 2015, and 2016.

[Negative values indicate net cooling from flow augmentation and positive values indicate net warming.]

Reach	Average temperature difference, in degrees Celsius																							
	2011								2015								2016							
	Apr	May	Jun	Jul	Aug	Sep	Oct	Season average	Apr	May	Jun	Jul	Aug	Sep	Oct	Season average	Apr	May	Jun	Jul	Aug	Sep	Oct	Season average
Augmented flow from Dexter Dam (Middle Fork Willamette River)																								
Springfield-McKenzie	0.0	0.0	0.0	-0.3	-0.5	-0.3	-0.2	-0.2	0.0	0.2	-0.1	0.0	0.0	0.3	0.5	0.1	-0.1	0.0	-0.1	-0.3	-0.1	0.5	0.2	0.0
McKenzie-Santiam	0.0	0.0	-0.1	-0.3	-0.5	-0.2	0.0	-0.2	0.0	-0.1	-0.3	-0.3	-0.1	0.3	0.5	0.0	-0.1	-0.1	-0.2	-0.3	-0.1	0.4	0.3	0.0
Santiam-Newberg	0.0	0.0	-0.1	-0.3	-0.4	-0.2	0.1	-0.1	0.0	-0.1	-0.3	-0.3	-0.2	0.1	0.2	-0.1	-0.1	-0.1	-0.2	-0.3	-0.2	0.2	0.1	-0.1
Newberg Pool	0.0	0.0	-0.1	-0.2	-0.4	-0.2	0.0	-0.1	0.0	-0.1	-0.2	-0.3	-0.2	0	0.2	-0.1	-0.1	-0.1	-0.1	-0.2	-0.2	0.1	0.1	-0.1
Willamette River	0.0	0.0	-0.1	-0.3	-0.5	-0.2	0.0	-0.1	0.0	-0.1	-0.3	-0.3	-0.1	0.2	0.3	0.0	-0.1	-0.1	-0.2	-0.3	-0.1	0.3	0.2	0.0
Augmented flow from Cougar Dam (South Fork McKenzie River)																								
Springfield-McKenzie	0.0	0.0	0.0	0.0	0.0	0.0	0.0	0.0	0.0	0.0	0.0	0.0	0.0	0.0	0.0	0.0	0.0	0.0	0.0	0.0	0.0	0.0	0.0	0.0
McKenzie-Santiam	-0.1	-0.1	-0.1	0.0	-0.2	-0.1	-0.4	-0.1	-0.3	-0.4	-0.2	-0.4	-0.3	-0.5	-0.6	-0.4	0.0	-0.1	0.0	-0.1	-0.3	-0.5	-0.2	-0.1
Santiam-Newberg	0.0	-0.1	-0.1	-0.1	-0.3	-0.1	-0.1	-0.1	-0.2	-0.2	-0.2	-0.4	-0.3	-0.3	-0.3	-0.3	0.0	-0.1	-0.1	-0.2	-0.3	-0.2	-0.1	-0.1
Newberg Pool	0.0	-0.1	-0.1	-0.1	-0.3	-0.1	-0.1	-0.1	-0.1	-0.2	-0.2	-0.3	-0.2	-0.2	-0.3	-0.2	0.0	-0.1	-0.1	-0.1	-0.2	-0.2	-0.1	-0.1
Willamette River	0.0	-0.1	-0.1	-0.1	-0.2	-0.1	-0.2	-0.1	-0.2	-0.3	-0.2	-0.4	-0.3	-0.3	-0.4	-0.3	0.0	-0.1	0.0	-0.1	-0.2	-0.3	-0.1	-0.1

Table 9. Monthly averaged difference in daily mean temperatures, by thermal reach, for uniform flow augmentation of 1,000 cubic feet per second over baseline conditions from Dexter (Middle Fork Willamette River), Cougar (South Fork McKenzie River), Foster (South Santiam River), or Big Cliff (North Santiam River) Dams, northwestern Oregon, compared to modeled baseline conditions in 2011, 2015, and 2016.—Continued

[Negative values indicate net cooling from flow augmentation and positive values indicate net warming.]

Reach	Average temperature difference, in degrees Celsius																							
	2011								2015								2016							
	Apr	May	Jun	Jul	Aug	Sep	Oct	Season average	Apr	May	Jun	Jul	Aug	Sep	Oct	Season average	Apr	May	Jun	Jul	Aug	Sep	Oct	Season average
Augmented flow from Foster Dam (South Santiam River)																								
Springfield-McKenzie	0.0	0.0	0.0	0.0	0.0	0.0	0.0	0.0	0.0	0.0	0.0	0.0	0.0	0.0	0.0	0.0	0.0	0.0	0.0	0.0	0.0	0.0	0.0	0.0
McKenzie-Santiam	0.0	0.0	0.0	0.0	0.0	0.0	0.0	0.0	0.0	0.0	0.0	0.0	0.0	0.0	0.0	0.0	0.0	0.0	0.0	0.0	0.0	0.0	0.0	0.0
Santiam-Newberg	0.0	0.0	-0.1	-0.4	-0.5	-0.3	-0.1	-0.2	-0.1	-0.3	-0.6	-0.8	-0.8	-0.4	0.0	-0.4	-0.1	-0.2	-0.4	-0.7	-0.8	-0.4	0.0	-0.4
Newberg Pool	0.0	0.0	-0.1	-0.3	-0.5	-0.3	-0.1	-0.2	-0.1	-0.3	-0.4	-0.6	-0.6	-0.4	-0.1	-0.3	-0.1	-0.2	-0.3	-0.5	-0.6	-0.4	-0.1	-0.3
Willamette River	0.0	0.0	-0.1	-0.2	-0.3	-0.2	-0.1	-0.1	-0.1	-0.2	-0.3	-0.4	-0.4	-0.2	0.0	-0.2	0.0	-0.1	-0.2	-0.3	-0.4	-0.2	0.0	-0.2
Augmented flow from Big Cliff Dam (North Santiam River)																								
Springfield-McKenzie	0.0	0.0	0.0	0.0	0.0	0.0	0.0	0.0	0.0	0.0	0.0	0.0	0.0	0.0	0.0	0.0	0.0	0.0	0.0	0.0	0.0	0.0	0.0	0.0
McKenzie-Santiam	0.0	0.0	0.0	0.0	0.0	0.0	0.0	0.0	0.0	0.0	0.0	0.0	0.0	0.0	0.0	0.0	0.0	0.0	0.0	0.0	0.0	0.0	0.0	0.0
Santiam-Newberg	-0.1	-0.1	-0.2	-0.4	-0.4	-0.2	-0.2	-0.2	-0.3	-0.5	-0.8	-0.9	-0.6	-0.3	-0.2	-0.5	-0.2	-0.3	-0.4	-0.5	-0.9	-0.6	-0.1	-0.4
Newberg Pool	-0.1	-0.1	-0.1	-0.3	-0.3	-0.2	-0.2	-0.2	-0.2	-0.4	-0.6	-0.7	-0.5	-0.2	-0.2	-0.4	-0.2	-0.3	-0.3	-0.4	-0.7	-0.5	-0.1	-0.3
Willamette River	0.0	-0.1	-0.1	-0.2	-0.2	-0.1	-0.1	-0.1	-0.1	-0.2	-0.4	-0.4	-0.3	-0.1	-0.1	-0.2	-0.1	-0.2	-0.2	-0.2	-0.4	-0.3	-0.1	-0.2

The effect of flow augmentation on water temperature in the Willamette River varied by season. Although the exact timing varies by year, the effect of flow augmentation generally was minimal in spring and peaked in July or August when main-stem Willamette River streamflows were typically at their lowest. Late summer and autumn streamflows tended to respond more variably to flow augmentation, depending on the temperature of release from upstream dams and reservoir water levels. Depending on the timing of seasonal cooling in the Willamette River, flow augmentation may provide some cooling through October (for example, in 2015). However, depending on the source and year, the effect of additional streamflow in autumn may be negligible. Notably, the effect of flow augmentation was not that of universal cooling, as might be expected based on a conceptual model of greater streamflow providing greater thermal mass. For example, increased releases from Lookout Point and Dexter Dams tended to warm the Willamette River in late summer and early autumn, an effect that was greatest in the Springfield-McKenzie and McKenzie-Santiam Reaches but persisted through all reaches to Willamette Falls (figs. 9–11; table 9). At times in 2011 and 2016, increased streamflow in the McKenzie River also caused transient warming downstream.

The source of flow augmentation and location of tributary confluence with the Willamette River influenced both the magnitude and extent of the downstream temperature effect. Of the four upstream-source scenarios modeled, flow augmentation in the Santiam River system (either North Santiam or South Santiam Rivers) caused the largest decrease in stream temperature in the Willamette River; however, the extent of this effect was limited to reaches of the Willamette River downstream from the Santiam River confluence. As an example, in July of 2015, flow augmentation sourced from Detroit Dam (and Big Cliff Dam) on the North Santiam River was modeled to reduce the average daily mean temperature of the Santiam-Newberg Reach by 0.9 °C and the Newberg Pool by 0.7 °C (table 9). In contrast, flow augmentation from Cougar Dam on the South Fork McKenzie River would have decreased temperatures in the Santiam-Newberg Reach and Newberg Pool by 0.4 and 0.3 °C, respectively. The McKenzie River, by nature of its confluence with the Willamette River farther upstream than the Santiam River, would also have reduced average July temperatures in the McKenzie-Santiam Reach by 0.4 °C, potentially decreasing temperatures in the thermally degraded section of river from the Calapooia River confluence (at Albany) to the Santiam River confluence (table 9; fig. 5), which is a reach that was unaffected by streamflow changes from the Santiam River. The Willamette River-averaged reduction in stream temperature resulting from flow augmentation sourced from Lookout Point and Dexter Dams on the Middle Fork Willamette River was the smallest of the four scenarios modeled in July of 2015 (table 9). However, this scenario was the only one modeled that was able to influence stream temperature in the full Willamette River.

Finally, distinct from differences caused by the source of flow augmentation, the thermal reaches of the Willamette River responded to changes in flow differently. As illustrated by longitudinal plots of the monthly averaged difference in daily mean temperature (fig. 12), the influence of additional streamflow on stream temperature varied both by source and by season; however, the pattern of downstream temperature response of the Willamette River to different flow-augmentation scenarios was similar across scenarios. In both the Springfield-McKenzie and McKenzie-Santiam Reaches, the difference in temperature due to flow augmentation generally increased with distance (fig. 12). Excluding the warm inflow from the Middle Fork Willamette River in September and October and the McKenzie River in June and July, greater cooling occurred with downstream distance. The temperature difference resulting from additional flow to either the Middle Fork Willamette or South Fork McKenzie Rivers was greatest (that is, most negative) immediately upstream from the Santiam River confluence with the Willamette River. Downstream from the Santiam River, however, the influence of flow augmentation on the Willamette River was approximately constant as far downstream as Rickreall Creek (RM 89.0), near Salem, then decreased with distance downstream to or through the Newberg Pool, depending on season. The effect of inflow from major tributaries reduced the influence of upstream flow augmentation by "diluting" the volume of augmentation, which comprises a smaller percentage of total streamflow downstream from major tributaries.

Temperature Conditions for Spring-Run Chinook Salmon

The temperature effects of increasing streamflow by 1,000 ft^3/s in various tributaries to the Willamette River can reduce the magnitude, duration, and extent of stressful conditions for cold-water salmonids, but the effect was relatively modest. Maximum daily stream temperature at a single model segment was reduced by as much as 1.7 °C (table 8) as a result of modeled flow augmentation, but a difference of this magnitude was limited to the more downstream portion of the Newberg Pool on a single day. Model results for this study showed that for July of 2015, the length of Willamette River within the study area classified as lethal for juvenile Chinook salmon would have been reduced by 6 to 8 percent using flow augmentation from one of four different sources, with augmentation in the Santiam River system slightly more effective than augmentation from tributaries farther upstream (tables 10, 11). Similarly, in August of 2011, flow augmentation from various sources was effective in reclassifying 5–8 percent of the Willamette River from adverse to optimal for juvenile Chinook salmon.

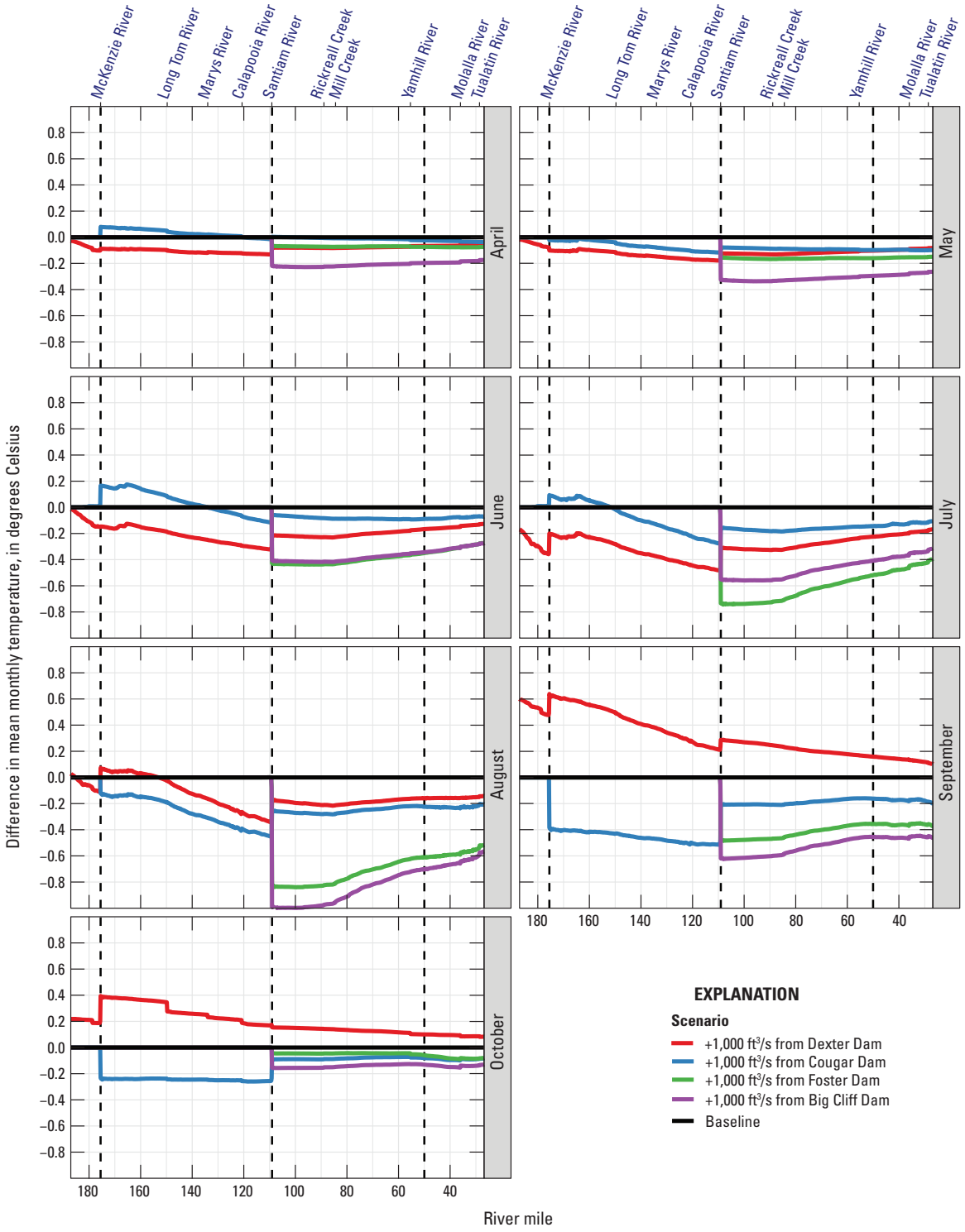

Figure 12. Monthly mean difference in daily mean modeled temperature in the Willamette River between baseline conditions and four flow-augmentation scenarios, northwestern Oregon, 2016. Rivers annotated on the x-axis are those included as tributaries in CE-QUAL-W2. Negative numbers indicate that the temperature is colder in the flow-augmentation scenario than under baseline conditions; positive numbers indicate that the temperature is warmer in the flow-augmentation scenario than under baseline conditions. Scenarios include additional flow from (1) Dexter Dam on the Middle Fork Willamette River, (2) Cougar Dam on the South Fork McKenzie River, (3) Foster Dam on the South Santiam River, and (4) Big Cliff Dam on the North Santiam River. Dashed vertical lines separate designated thermal reaches, from upstream to downstream: (1) Springfield-McKenzie Reach, (2) McKenzie-Santiam Reach, (3) Santiam-Newberg Reach, and (4) Newberg Pool.

Table 10. Monthly averaged difference in percent of Willamette River length (head to Willamette Falls) classified into thermal stress categories for juvenile Chinook salmon, for uniform flow augmentation of 1,000 cubic feet per second from Dexter (Middle Fork Willamette River), Cougar (South Fork McKenzie River), Foster (South Santiam River), or Big Cliff (North Santiam River) Dams in northwestern Oregon compared to modeled baseline conditions in 2011, 2015, and 2016.

[Negative values indicate net cooling from flow augmentation and positive values indicate net warming. See table 2 for definition of temperature ranges for the thermal categories.]

Thermal category	Percentage difference																			
	2011							2015							2016					
	Apr	May	Jun	Jul	Aug	Sep	Oct	Apr	May	Jun	Jul	Aug	Sep	Oct	Apr	May	Jun	Jul	Aug	Sep	Oct
Augmented flow from Dexter Dam (Middle Fork Willamette River)																				
Lethal	0	0	0	0	0	0	0	0	0	-1	-6	-1	0	0	0	0	0	-1	0	0	0
Adverse	0	0	0	-3	-8	0	0	0	-1	-5	4	-1	0	0	0	0	-3	-5	-2	0	0
Optimal	-1	-1	0	3	8	0	0	2	1	6	2	2	0	0	-1	0	3	6	2	0	0
Suboptimal	1	1	0	0	0	0	0	-2	0	0	0	0	0	0	1	0	0	0	0	0	0
Augmented flow from Cougar Dam (South Fork McKenzie River)																				
Lethal	0	0	0	0	0	0	0	0	0	-1	-7	-1	0	0	0	0	0	-1	0	0	0
Adverse	0	0	0	-2	-5	0	0	0	-1	-4	3	-4	-4	0	0	0	-1	-2	-4	0	0
Optimal	-1	-3	0	2	5	0	0	-3	1	5	4	4	4	0	0	0	1	3	4	0	0
Suboptimal	1	3	0	0	0	0	0	3	0	0	0	0	0	0	0	0	0	0	0	0	0
Augmented flow from Foster Dam (South Santiam River)																				
Lethal	0	0	0	0	0	0	0	0	0	-2	-8	-1	0	0	0	0	0	-2	-1	0	0
Adverse	0	0	0	-3	-8	0	0	0	-2	-3	5	-4	-3	0	0	0	-2	-3	-3	0	0
Optimal	0	-1	0	3	8	0	0	0	2	5	3	5	3	0	0	0	2	5	4	0	0
Suboptimal	0	1	0	0	0	0	0	0	0	0	0	0	0	0	0	0	0	0	0	0	0
Augmented flow from Big Cliff Dam (North Santiam River)																				
Lethal	0	0	0	0	0	0	0	0	0	-2	-8	-1	0	0	0	0	0	-2	-1	0	0
Adverse	0	0	0	-4	-7	0	0	0	-2	-4	5	-1	-2	0	0	0	-2	-2	-4	0	0
Optimal	-1	-2	0	4	7	0	0	-2	2	6	3	3	2	0	-1	0	2	4	4	0	0
Suboptimal	1	2	0	0	0	0	0	2	0	0	0	0	0	0	1	0	0	0	0	0	0

Table 11. Length of Willamette River (head to Willamette Falls) within designated temperature range for juvenile Chinook salmon rearing and growth grouped by month, as percent, with uniform low augmentation of 1,000 cubic feet per second from Dexter (Middle Fork Willamette River), Cougar (South Fork McKenzie River), Foster (South Santiam River), or Big Cliff (North Santiam River) Dams in northwestern Oregon compared to modeled baseline conditions in 2011, 2015, and 2016.

[See table 2 for definition of temperature ranges for the thermal categories.]

Thermal category	Percentage of modeled river length																				
	2011							2015							2016						
	Apr	May	Jun	Jul	Aug	Sep	Oct	Apr	May	Jun	Jul	Aug	Sep	Oct	Apr	May	Jun	Jul	Aug	Sep	Oct
Augmented flow from Dexter Dam (Middle Fork Willamette River)																					
Lethal	0	0	0	0	0	0	0	0	0	1	11	3	0	0	0	0	0	1	0	0	0
Adverse	0	0	0	4	16	0	0	0	2	54	72	73	8	0	0	0	14	51	66	1	0
Optimal	11	78	99	96	84	100	100	94	98	45	16	24	92	100	96	100	86	48	34	99	100
Suboptimal	89	22	1	0	0	0	0	6	0	0	0	0	0	0	4	0	0	0	0	0	0
Augmented flow from Cougar Dam (South Fork McKenzie River)																					
Lethal	0	0	0	0	0	0	0	0	0	1	11	3	0	0	0	0	0	1	0	0	0
Adverse	0	0	0	5	18	0	0	0	2	55	72	70	5	0	0	0	16	54	63	1	0
Optimal	11	76	99	95	82	100	100	89	98	44	18	26	95	100	96	100	84	45	37	99	100
Suboptimal	89	24	1	0	0	0	0	11	0	0	0	0	0	0	4	0	0	0	0	0	0
Augmented flow from Foster Dam (South Santiam River)																					
Lethal	0	0	0	0	0	0	0	0	0	0	10	3	0	0	0	0	0	0	0	0	0
Adverse	0	0	0	4	15	0	0	0	1	56	74	70	5	0	0	0	15	53	64	1	0
Optimal	13	78	99	96	85	100	100	92	99	44	17	27	95	100	97	100	85	47	36	99	100
Suboptimal	87	22	1	0	0	0	0	8	0	0	0	0	0	0	4	0	0	0	0	0	0
Augmented flow from Big Cliff Dam (North Santiam River)																					
Lethal	0	0	0	0	0	0	0	0	0	0	9	3	0	0	0	0	0	0	0	0	0
Adverse	0	0	0	3	17	0	0	0	1	55	74	72	6	0	0	0	15	54	63	0	0
Optimal	11	77	99	97	83	100	100	90	99	45	17	25	94	100	96	100	85	46	37	100	100
Suboptimal	89	23	1	0	0	0	0	10	0	0	0	0	0	0	4	0	0	0	0	0	0

Flow augmentation tended to improve lethal or adverse temperature conditions for Chinook salmon by reducing the upstream extent and duration of challenging thermal conditions (fig. 13). Modeling results showed that flow augmentation in all four scenarios would have reduced or prevented several days of lethal conditions in the Santiam-Newberg Reach and the Newberg Pool in late July and reduced the upstream extent of lethal conditions in early July and August of 2015, the most extreme hydroclimatological year in the study. Notably, where this reduction occurred varied by scenario. When augmenting streamflow via the Middle Fork Willamette or South Fork McKenzie Rivers, lethal conditions occurring from approximately Albany to the Marys River confluence would have been prevented. In contrast, augmenting additional flow via the North Santiam or South Santiam Rivers would have prevented lethal conditions in the uppermost reaches of the Santiam-Newberg Reach but would have had no effect on lethal conditions in the lower portions of the McKenzie-Santiam Reach.

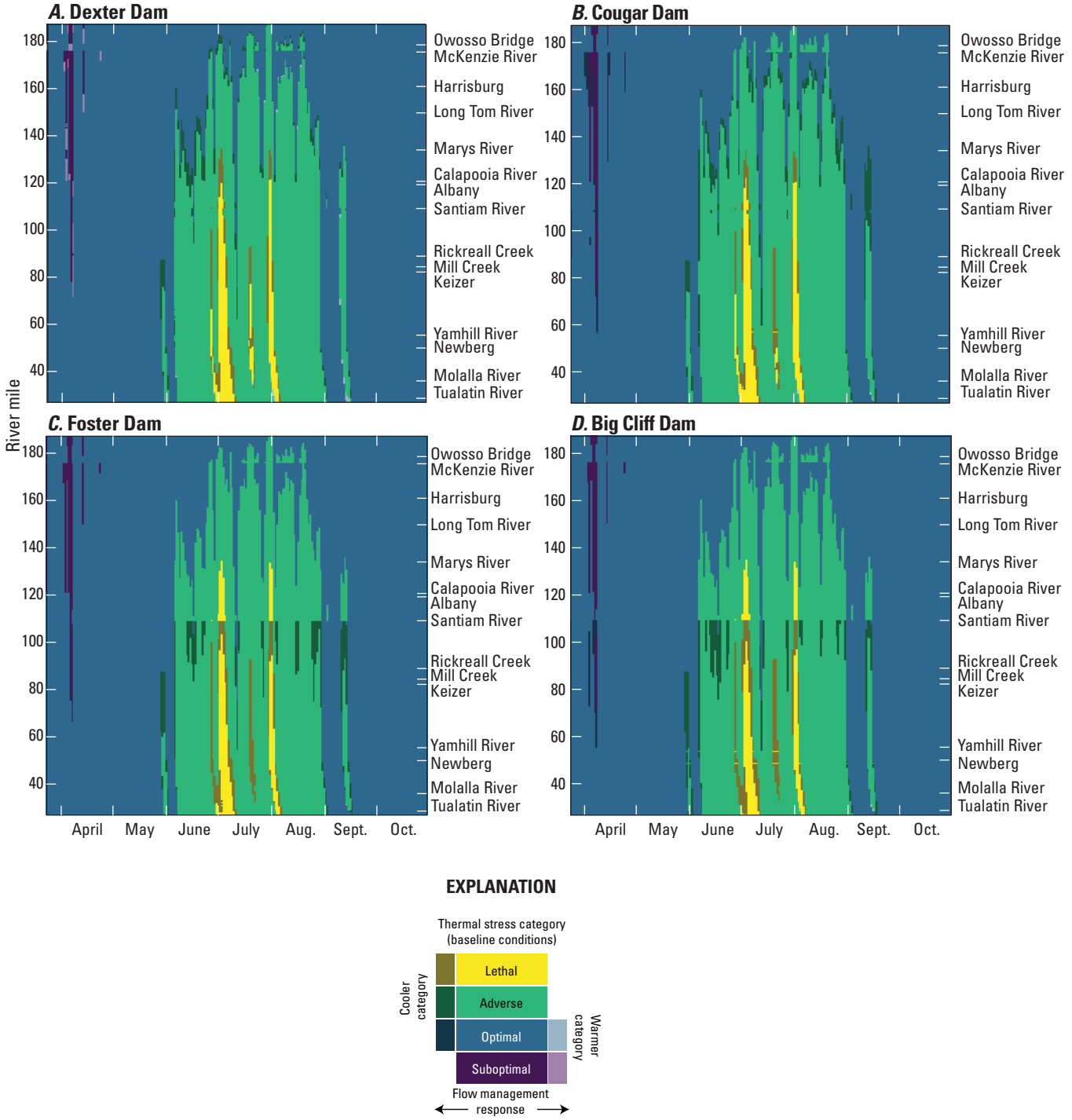

Figure 13. Thermal stress category for juvenile Chinook salmon (*Oncorhynchus tshawytscha*) under baseline conditions in 2015 overlain by any change in thermal category as the result of 1,000 cubic feet per second added to baseline conditions sourced from (*A*) Dexter Dam on the Middle Fork Willamette River, (*B*) Cougar Dam on the South Fork McKenzie River, (*C*) Foster Dam on the South Santiam River, or (*D*) Big Cliff Dam on the North Santiam River, northwestern Oregon. Colors in the "warmer category" (lighter) indicate that the model segment was classified as a more-stressful category for juvenile Chinook salmon under the flow-augmentation scenario than under baseline conditions (for example, a baseline category of "adverse" overlain by a flow-augmentation scenario category of "lethal".); colors in the "cooler category" indicate that the model segment was classified as a less-stressful category for juvenile Chinook salmon under the flow-augmentation scenario than under baseline conditions (for example, a baseline category of "adverse" overlain by a flow-augmentation scenario category of "optimal.").

Discussion

The idealized conceptual model of longitudinal thermal patterns in streams is one of asymptotic downstream warming, where cool headwaters warm non-linearly until reaching a dynamic "pseudo equilibrium" with air temperature in the lower reaches of a stream (Vannote and others, 1980; Bogan and others, 2003; Caissie, 2006). Although many examples have shown this paradigm to be oversimplified (Dent and others, 2008; Fullerton and others, 2015; Arora and others, 2018), the nature of the deviation of a stream from an asymptotic warming profile can provide insight into the underlying controls on stream temperature.

In a general sense, the Willamette River upstream from Willamette Falls was consistent with the asymptotic warming paradigm. In summer, the river tended to be coolest upstream and to warm downstream, with the steepest rate of downstream warming in the Springfield-McKenzie Reach and progressively smaller warming rates farther downstream. In the upper reaches during summer, the Willamette River was both shallower and further from its theoretical equilibrium temperature, resulting in a larger net positive heat flux than what was modeled downstream, where the river was both closer to its equilibrium temperature and deeper. (A shallow river reach will warm faster than a deeper reach of the same temperature when exposed to the same surface heat fluxes.) This pattern was probably enhanced by the longitudinal changes in the geomorphology of the Willamette River. The river is more laterally dynamic in its upper reaches, with actively shifting gravel bars, areas of local bank erosion and some multithreaded sections, whereas downstream the channel is single-threaded, deeper, laterally stable, and has fewer gravel bars (Wallick and others, 2013). While multi-threaded reaches with gravel bars can theoretically insulate streams from heating as the result of shading from riparian vegetation and enhanced hyporheic flow, increased relative exposure to surface heating can cause rapid heating where these processes are limited (Mosley, 1983; Caissie, 2006).

Tributaries to the Willamette River tended to create discontinuities in the longitudinal thermal profile, but the effect varied by season, variations in dam operations, and other local factors influencing the heat budgets of individual tributary streams. Smaller streams draining the Coast Range or the lower Cascade Range foothills (for example, the Yamhill or Calapooia Rivers), which do not receive much input from snowmelt or cold groundwater from High Cascades springs, tended to warm the Willamette River. However, the influence of these streams, which lack upstream reservoir storage, tended to be both minor and seasonally limited. In spring, when streamflows were high, small tributaries to the Willamette River may influence its downstream temperature by tenths of a degree Celsius, but the effect tended to be negligible during the summer low-flow season (figs. 3, 4). In contrast, the confluence of the McKenzie and Santiam Rivers with the Willamette River typically caused large discontinuities in the thermal profile across all modeled seasons from spring through autumn. Relative to other streams in the Willamette River Basin, both the McKenzie and Santiam Rivers maintained relatively high streamflow throughout the summer. This effect was the influence of both naturally stable streamflow influenced by High Cascades springs in their headwaters as well as flow augmentation from reservoir storage. With some variation by year, the McKenzie River, which derives a large proportion of its streamflow from High Cascades springs and thus tends to be both hydrologically and thermally stable relative to other tributaries in the Willamette River Basin (Tague and others, 2007; Risley and others, 2010), tended to warm the Willamette River in spring and to cool it in summer and autumn.

All reaches of the Willamette River were directly influenced by the temperature of dam releases upstream, but the effect diminished with time, distance, and the influx of other tributaries (Rounds, 2010; Arora and others, 2018; Rounds and Stratton Garvin, 2022). Dexter Dam is only 16.5 miles upstream from the head of the Willamette River; thus, the Springfield-McKenzie Reach of the Willamette River upstream from the McKenzie River confluence is strongly controlled by the temperature of water released from Dexter Dam. The release of accumulated summer-heated water in Lookout Point and Dexter Lakes in autumn (Rounds, 2010) caused temperatures in the Springfield-McKenzie Reach of the Willamette River to be anomalously warm. By October, much of the Willamette River was relatively isothermal except for the Springfield-McKenzie Reach upstream from the McKenzie River confluence, which may be several degrees Celsius warmer than the rest of the Willamette River (figs. 3, 4).

The combined effects of the influence of local geomorphic controls, major tributaries, and upstream dam releases produced a complex longitudinal thermal profile in the Willamette River. In a general sense, the river warmed in the downstream direction; however, the lower sections of the Springfield-McKenzie and McKenzie-Santiam Reaches had higher temperatures than those downstream from the McKenzie and Santiam River confluences, respectively. From about RM 120 near Albany to the confluence with the Santiam River, the cumulative July and August heat content was only slightly smaller than that in the lower reaches of the Santiam-Newberg Reach as far downstream as RM 50 (fig. 5). Additionally, on a daily basis, the warmest part of the river model domain cannot be assumed to be at Willamette Falls. At the start of a heat wave, the highest daily maximum temperatures in the river were probably near the end of the Santiam-Newberg Reach, where longitudinal heating remained strong, and the river was shallow enough to still respond relatively quickly to weather conditions. As the heat wave persisted and then waned, peak temperatures continued to travel through the Newberg Pool for several days after the rest of the river began to cool (fig. 3).

Model results showed that thermally unfavorable conditions for juvenile and adult Chinook salmon in the Willamette River upstream from Willamette Falls were chronic and extensive during the summer. Adverse conditions for juvenile Chinook salmon extended through the Newberg Pool, the

Santiam-Newberg Reach, and into the McKenzie-Santiam Reach during peak heating in 2011, and into all four defined thermal reaches of the Willamette River in 2015 and 2016. In 2015, adverse or lethal conditions were present well upstream from the Santiam River confluence from early June to September. Conditions in 2016 were less extreme, with adverse conditions present for most of July and August and lethal conditions present during heat waves (figs. 7, 8). The results from a uniform flow augmentation of 1,000 ft^3/s suggested that the effect of this magnitude of additional streamflow was limited in terms of reducing the occurrence of chronically adverse conditions, but that this level of flow augmentation can reduce (or eliminate, in limited instances) the extent and duration of lethal conditions in the Willamette River. For example, although flow augmentation reduced the reach-averaged, monthly averaged stream temperatures in the Willamette River upstream from Willamette Falls by a maximum of only 0.9 °C in July of 2015, this resulted in a reduction in the linear extent of lethal conditions for juvenile Chinook salmon from 17 percent to 9 percent, almost cutting that occurrence in half (tables 9, 10). As shown in figure 13, this temperature decrease translated to the effective elimination of lethal conditions in the Santiam-Newberg Reach and the upstream portion of the Newberg Pool during a short-duration heat wave in late July of 2015.

Flow augmentation to the North Santiam or South Santiam Rivers from Detroit/Big Cliff or Green Peter/Foster Dams, respectively, had a larger effect on temperatures immediately downstream from the Santiam River confluence with the Willamette River than did flow augmentation to the McKenzie or Middle Fork Willamette Rivers at their respective confluences with the Willamette River. This finding may be somewhat counterintuitive, as 1,000 ft^3/s constituted a smaller percentage of total streamflow in the Willamette River downstream from the Santiam River confluence than farther upstream. However, comparison of the baseline and augmented-flow scenario temperatures of the Santiam, McKenzie, and Middle Fork Willamette Rivers immediately upstream from their confluence with the Willamette River suggested that, assuming no change in the temperature of dam releases, flow augmentation to the North Santiam or South Santiam River lowered the temperature of the Santiam River but not of the McKenzie or Middle Fork Willamette Rivers immediately upstream from their confluence with the Willamette River (fig. 14). The combination of lower temperature with greater streamflow entering the Willamette River compounded the effect of flow augmentation entering the Willamette River from the Santiam River system in a way not replicated by the Middle Fork Willamette or McKenzie Rivers. A possible explanation for this pattern was that in the Santiam River system, flow augmentation reduced the rate of longitudinal warming for the 48.3 or 58.6 river miles from Foster and Big Cliff Dams, respectively, to the Willamette River confluence. In contrast, the 16.5 river miles from Dexter Dam to the head of the Willamette River, at the confluence of the Coast Fork Willamette and Middle Fork Willamette Rivers, is relatively short, which caused the advected heat released from Dexter Dam to remain the dominant influence on temperatures in the Middle Fork Willamette River and uppermost Willamette River. Finally, the South Fork McKenzie River contributed a relatively small portion of the streamflow to the McKenzie River, limiting its influence on downstream temperatures in the McKenzie and Willamette Rivers. Confirmation of these hypotheses, as well as a better understanding of the thermal effects of flow augmentation within the tributaries to the Willamette River, could be investigated in future studies using the CE-QUAL-W2 models applied in this study.

Finally, results from the flow-augmentation scenarios in this study suggested that, except during low-flow years with an early and particularly warm summer (such as 2015), flow augmentation to manage thermal stress to threatened fish populations was most effective for short periods in mid- to late-summer (July through August and sometimes into September), when annual temperatures were high and flows were low. In April, May, and June, the monthly averaged difference in daily mean temperatures across flow-augmentation scenarios and reaches (with a few exceptions; for example, June of 2015) were in the range of 0.1–0.2 to a maximum of 0.4 °C (table 9). The effect in July and August tended to be several tenths of a degree greater. In years like 2015, when spring flows were relatively low, however, flow augmentation earlier in the year may have greater influence on stream temperatures. Depending on reservoir, streamflow, and weather conditions, flow augmentation into September may also be similarly effective in reducing peak temperatures (figs. 9–11). These results suggested that targeted use of flow-management strategies to reduce thermally stressful conditions for threatened cold-water salmonids are likely to be most effective during the hottest days of summer but may provide limited thermal benefit in spring months when flows are low. However, to better anticipate the likely magnitude of cooling (in terms of total temperature change, and the spatial area over which those changes might occur), additional modeling is needed wherein different reservoir and hydroclimatological conditions are paired with viable dam operation scenarios.

Study Limitations

Compared to field-based studies, the water-temperature models presented within this report can provide a better understanding of both the spatial and temporal variability of stream temperature and provide insight into the thermal response of a river to specific actions, such as flow augmentation. However, the results from this study should be interpreted with care. Modeling performed using CE-QUAL-W2 is limited to the simplified main channel of the Willamette River and those processes simulated by CE-QUAL-W2 at a “reach scale” of about 500 m. The model does not simulate lateral temperature variations, smaller habitat-scale variability, or the conditions in off-channel features, which may vary from the main channel of the Willamette River by many degrees Celsius

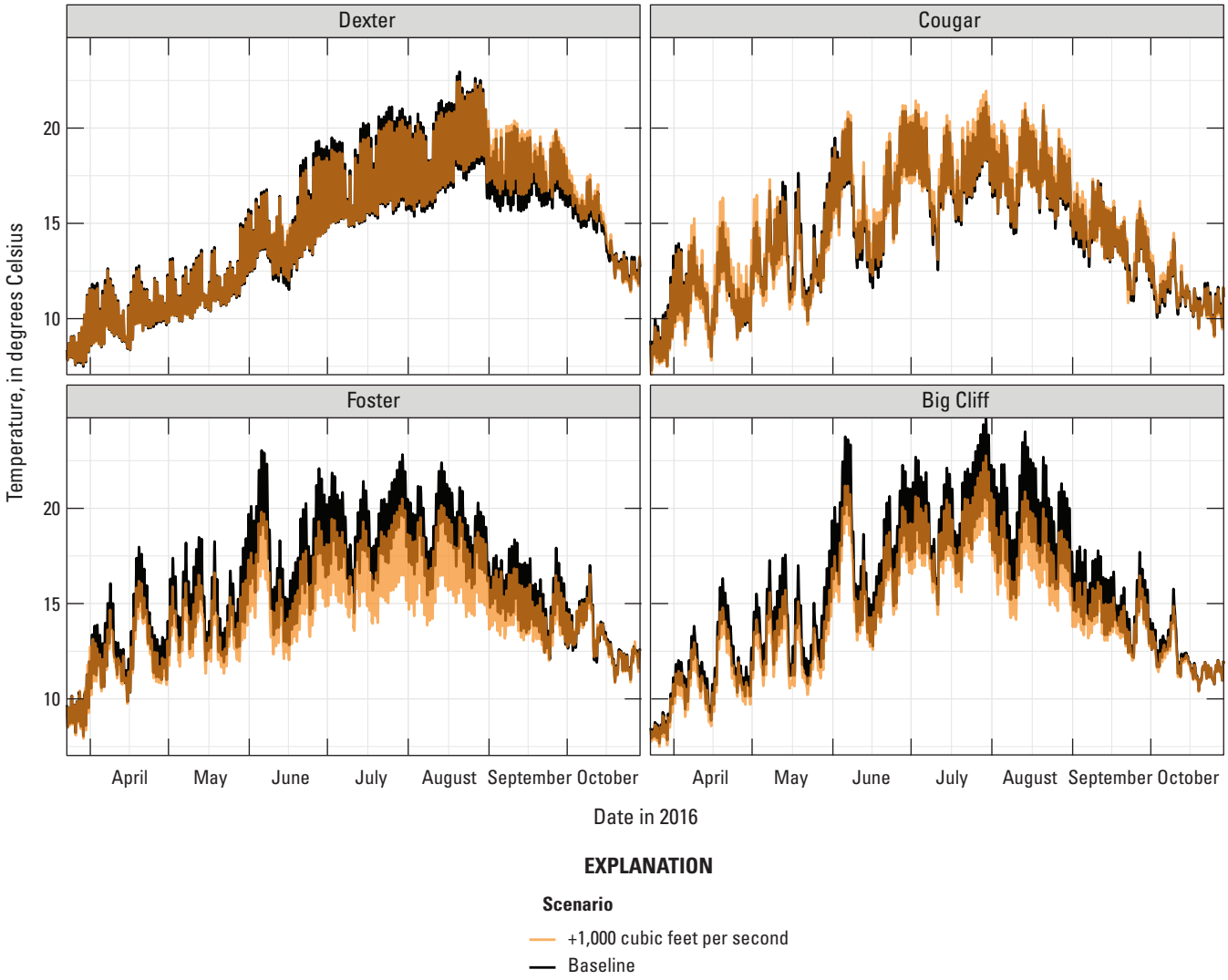

Figure 14. Comparison of modeled water temperatures in tributaries just upstream from their confluence with the Willamette River, northwestern Oregon. (A) Middle Fork Willamette River downstream from releases from Dexter Dam; (B) McKenzie River downstream from releases from Cougar Dam; (C) Santiam River downstream from releases from Foster Dam; and (D) the Santiam River downstream from releases from Big Cliff Dam in baseline and flow augmented (+1,000 cubic feet per second) scenarios, 2016.

(Torgersen and others, 2012; Gombert, 2018; Mangano and others, 2018; Smith and others, 2020). Furthermore, although the net effect of groundwater discharge and recharge are included in the Willamette River models implicitly as a "distributed tributary" (averaged inflow or outflow applied across a model branch), the effects of hyporheic flows are not explicitly modeled in CE-QUAL-W2.

The flow-augmentation scenarios were intended to be a sensitivity analysis to establish the magnitude, timing, and extent of streamflow influence on stream temperature. The scenarios run in this study do not account for dam-specific management actions, such as changing the balance of water releases from one dam outlet to another. Additionally, increasing dam releases by 1,000 ft^3/s for a sustained period would alter the thermal structure of the reservoir behind the dam, thus altering the temperature of those releases. Because water released from Detroit/Big Cliff, Green Peter/Foster, or Cougar Dams traveled many miles in tributary streams while exchanging heat with the surrounding environment prior to reaching the Willamette River, the effect of dam-release temperatures on downstream modeled Willamette River temperatures for these scenarios was somewhat limited. However, the effect of an altered thermal structure in Lookout Point Lake, resulting from sustained higher releases to the Middle Fork Willamette River on the temperature of the Springfield-McKenzie Reach of the Willamette River, may be more substantial.

Finally, the modeled flow-augmentation scenarios did not include any calculations to determine whether sufficient stored water was indeed available for release. Flow augmentation of 1,000 ft^3/s released for one day is equivalent to about 1,983 acre-feet of stored water, or the daily use of approximately 0.6 percent of total conservation storage in Lookout Point

Lake and 18 percent of total conservation storage in Lookout Point Lake in one month (National Marine Fisheries Service, 2008). In Cougar Reservoir, 1,983 acre-ft/day accounts for approximately 1 percent of storage usage per day, or 39 percent in a month. In 2015 and 2016, when the reservoirs of the Willamette Valley Project did not fill (U.S. Army Corps of Engineers, 2020), an additional release of 1,000 ft^3/s may have been sustainable for only a limited number of days.

Conclusions and Future Work

Modeling performed using CE-QUAL-W2 produced a detailed characterization of stream temperature in both space and time at scales not easily replicable with a data-based study, allowing a multi-faceted assessment of the thermal landscape of the Willamette River system. Continuous temperature monitors in the Willamette River showed that the river tended to warm downstream during summer (U.S. Geological Survey, 2020) and those warm temperatures represented adverse conditions for cold-water salmonids. However, the model results from this study provided a more complex portrait of the downstream evolution of river temperatures. Downstream warming rates were greatest in summer but varied along four characteristic "thermal reaches" and with the influx from major dammed tributaries. The resulting longitudinal temperature profile indicated that the Willamette River upstream from Willamette Falls was not always warmest at more-downstream locations; in some upstream reaches such as the reach from Albany to the Santiam River confluence, temperatures and cumulative degree-day heating may be comparable to reaches many miles downstream. Except in cool, wet years such as 2011, adversely warm conditions for spring-run Chinook salmon were extensive for much of June or July through August in the Willamette River. Flow augmentation at the scale of 1,000 ft^3/s can be effective in reducing the occurrence, duration, and extent of lethally warm temperatures during the summer low-flow season but was limited in reducing the extent or duration of adversely warm conditions. Furthermore, the magnitude and direction (cooling or warming) of the thermal effects of flow augmentation varied by tributary source and season. During spring, when streamflow was high and stream temperatures were generally cooler, the influence of 1,000 ft^3/s on stream temperature was muted compared to later in summer, when streamflow was lower and stream temperatures were higher. In autumn, flow augmentation from dams on the South Fork McKenzie, South Santiam, or North Santiam Rivers produced a cooling effect on the Willamette River. However, increased releases from Lookout Point and Dexter Dams on the Middle Fork Willamette River (only 16.5 miles upstream from the head of the Willamette River) caused a net warming effect due to the export of an accumulation of heat stored in Lookout Point Lake during the summer and the proximity of Dexter Dam to the Willamette River (especially in warmer years like 2015 and 2016). While greatest in the upstream reaches of the Willamette River, this warming effect during autumn was propagated throughout the entire modeling domain as far downstream as Willamette Falls.

This study provided a multifaceted investigation of seasonal, annual, and spatial patterns in stream temperature in the Willamette River, but many questions regarding flow management and river water temperature remain. While beyond the scope of this study, future investigations into the temperature dynamics of the major tributaries to the Willamette River could provide greater insights into both the controls on stream temperature and management options for improving thermal conditions for threatened salmonids. Similarly, more focused and specific investigations into individual flow-management actions at large dams (for example, strategies for the use of various dam outlets, the use of different release-temperature targets, or the effectiveness of structural outlet modifications), and the effects of such actions on the thermal landscape of the tributaries and the Willamette River are necessary to better understand the potential to improve thermal conditions for threatened fish populations in the Willamette River Basin. This study investigated those thermal effects only for juvenile rearing and growth and adult migration in Chinook salmon, excluding both adult spawning and all life-stages of winter-run steelhead. To better understand the thermal effects of Willamette River conditions on aquatic species, the effects on other life stages and other keys species would need to be investigated, and a better understanding of other facets of the temperature regime may provide additional insights. For example, continuous temperature monitoring in the Willamette River suggested that the upper reaches of the river tended to exhibit a greater diurnal variability than the lower reaches (U.S. Geological Survey, 2020), which may provide longer "resting periods" for fish exposed to chronic or acute thermal stress. Likewise, thermal diversity not captured by a main-channel-exclusive modeling study such as this may be critical to the aquatic health of sensitive species. While many individual studies of water quality in off-channel environments have been completed on the Willamette River, an integrated and holistic understanding of thermal diversity across all wetted environments of the Willamette River system remains to be developed.

Acknowledgments

The authors thank Norm Buccola, Rich Piaskowski, Greg Taylor, and Jake Macdonald of the U.S. Army Corps of Engineers; Stan Gregory and Tyrell Deweber of Oregon State University; Rose Wallick, James White, Toby Kock, Gabe Hansen, Russ Perry, Krista Jones and Jim Peterson of the U.S. Geological Survey, and others involved in the "SWIFT" process for their vision and support in developing this study. The authors also thank Toby Kock, Russ Perry, and Gabe Hansen of the U.S. Geological Survey for their work summarizing the salmonid temperature thresholds.

References Cited

Annear, R., McKillip, M., Khan, S.J., Berger, C., and Wells, S., 2004, Willamette River Basin temperature TMDL model—Boundary conditions and model setup: Department of Civil and Environmental Engineering, Portland State University, Oregon, Technical Report EWR-01-04, 530 p.

Arora, R., Toffolon, M., Tockner, K., and Venohr, M., 2018, Thermal discontinuities along a lowland river—The importance of urban areas and lakes: Journal of Hydrology, v. 564, p. 811–823, accessed January 9, 2021, at https://doi.org/10.1016/j.jhydrol.2018.05.066.

Berger, C., McKillip, M., Annear, R., Khan, S.J., and Wells, S., 2004, Willamette River Basin temperature TMDL model—Model calibration: Department of Civil and Environmental Engineering, Portland State University, Oregon, 341 p.

Bloom, J.R., 2016, South Santiam River, Oregon, hydrodynamics and water temperature modeling, 2000–2002: Portland, Oregon Department of Environmental Quality, 53 p.

Bogan, T., Mohseni, O., and Stefan, H.G., 2003, Stream temperature-equilibrium temperature relationship: Water Resources Research, v. 39, no. 9, accessed January 9, 2021, at https://doi.org/10.1029/2003WR002034.

Brett, J.R., Clarke, W.C., and Shelbourn, J.E., 1982, Experiments on thermal requirements for growth and food conversion efficiency of juvenile Chinook salmon, *Oncorhynchus tshawytscha*: Canadian Technical Report of Fisheries and Aquatic Sciences, v. 1127, p. 1–29.

Brown, G.W., 1969, Predicting temperatures of small streams: Water Resources Research, v. 5, no. 1, p. 68–75, accessed January 9, 2021, at https://doi.org/10.1029/WR005i001p00068.

Buccola, N.L., Rounds, S.A., Sullivan, A.B., and Risley, J.C., 2012, Simulating potential structural and operational changes for Detroit Dam on the North Santiam River, Oregon, for downstream temperature management: U.S. Geological Survey Scientific Investigations Report 2012–5231, 68 p. [Also available at https://doi.org/10.3133/sir20125231.]

Buccola, N.L., 2017, Water temperature effects from simulated changes to dam operations and structures in the Middle and South Santiam Rivers, Oregon: U.S. Geological Survey Open-File Report 2017–1063, 19 p. [Also available at https://doi.org/10.3133/ofr20171063.]

Buccola, N.L., Stonewall, A.J., and Rounds, S.A., 2015, Simulations of a hypothetical temperature control structure at Detroit Dam on the North Santiam River, northwestern Oregon: U.S. Geological Survey Open-File Report 2015–1012, 30 p. [Also available at https://doi.org/10.3133/ofr20151012.]

Burkholder, B.K., Grant, G.E., Haggerty, R., Khangaonkar, T., and Wampler, P.J., 2008, Influence of hyporheic flow and geomorphology on temperature of a large, gravel-bed river, Clackamas River, Oregon, USA: Hydrological Processes, v. 22, no. 7, p. 941–953, accessed January 9, 2021, at https://doi.org/10.1002/hyp.6984.

Caissie, D., 2006, The thermal regime of rivers—A review: Freshwater Biology, v. 51, no. 8, p. 1389–1406, accessed January 9, 2021, at https://doi.org/10.1111/j.1365-2427.2006.01597.x.

Conlon, T.D., Wozniak, K.C., Woodcock, D., Herrera, N.B., Fisher, B.J., Morgan, D.S., Lee, K.K., and Hinkle, S.R., 2005, Ground-water hydrology of the Willamette Basin, Oregon: U.S. Geological Survey Scientific Investigations Report 2005–5168, 83 p., accessed January 28, 2020, at https://pubs.usgs.gov/sir/2005/5168/.

Dent, L., Vick, D., Abraham, K., Schoenholtz, S., and Johnson, S., 2008, Summer temperature patterns in headwater streams of the Oregon Coast range: Journal of the American Water Resources Association, v. 44, no. 4, p. 803–813, accessed January 9, 2021, at https://doi.org/10.1111/j.1752-1688.2008.00204.x.

Dykaar, B.B. and Wigington, P.J., Jr., 2000, Floodplain formation and cottonwood colonization patterns on the Willamette River, Oregon, USA: Environmental Management, v. 25, no. 1, p. 87–104, accessed January 9, 2021, at https://doi.org/10.1007/s002679910007.

Fullerton, A.H., Torgersen, C.E., Lawler, J.J., Faux, R.N., Steel, E.A., Beechie, T.J., Ebersole, J.L., and Leibowitz, S.G., 2015, Rethinking the longitudinal stream temperature paradigm—Region-wide comparison of thermal infrared imagery reveals unexpected complexity of river temperatures: Hydrological Processes, v. 29, no. 22, p. 4719–4737, accessed January 9, 2021, at https://doi.org/10.1002/hyp.10506.

Gombert, C.E., 2018, Characterization of thermal regimes of side channels, alcoves, and ponds on the Willamette River, OR: Oregon State University master's thesis, 141 p.

Gregory, S., Ashkenas, L., and Nygaard, C., 2007a, Summary report to assist development of ecosystem flow recommendations for the Middle Fork and Coast Fork of the Willamette River, Oregon: Corvallis, Oregon State University, Institute for Water and Watersheds, 237 p.

Gregory, S., and Wildman, R., l, Hulse, D., Ashkenas, L., and Boyer, K., 2007b, Historical changes in hydrology, geomorphology, and floodplain vegetation of the Willamette River, Oregon: River Research and Applications, v. 35, no. 8, p. 1279–1290, accessed January 9, 2021, at https://onlinelibrary.wiley.com/doi/abs/10.1002/rra.3495.

Hansen, A.C., Kock, T.J., and Hansen, G.S., 2017, Synthesis of downstream fish passage information at projects owned by the U.S. Army Corps of Engineers in the Willamette River Basin, Oregon: U.S. Geological Survey Open File Report 2017–1101, 118 p., accessed January 9, 2021, at https://doi.org/10.3133/ofr20171101.

International Commission on Large Dams, 2011, Constitution: France, International Commission on Large Dams, 21 p., accessed November 30, 2020, at https://www.icold-cigb.org/userfiles/files/CIGB/INSTITUTIONAL_FILES/Constitution2011.pdf.

Jefferson, A., Grant, G., and Rose, T., 2006, Influence of volcanic history on groundwater patterns on the west slope of the Oregon High Cascades: Water Resources Research, v. 42, no. 12, W12411, accessed January 9, 2021 at https://doi.org/10.1029/2005WR004812.

Johnson, S.L., 2004, Factors influencing stream temperatures in small streams—Substrate effects and a shading experiment: Canadian Journal of Fisheries and Aquatic Sciences, v. 61, no. 6, p. 913–923, accessed January 9, 2021, at https://doi.org/10.1139/f04-040.

Keefer, M.L., Taylor, G.A., Garletts, D.F., Gauthier, G.A., Pierce, T.M., and Caudill, C.C., 2010, Prespawn mortality in adult spring Chinook salmon outplanted above barrier dams: Ecology Freshwater Fish, v. 19, no. 3, p. 361–372, accessed January 9, 2021, at https://doi.org/10.1111/j.1600-0633.2010.00418.x.

Leach, J.A., Olson, D.H., Anderson, P.D., and Eskelson, B.N.I., 2017, Spatial and seasonal variability of forested headwater stream temperatures in western Oregon, USA: Aquatic Sciences, v. 79, no. 2, p. 291–307, accessed January 9, 2021, at https://doi.org/10.1007/s00027-016-0497-9.

Mangano, J.F., Piatt, D.R., Jones, K.L, and Rounds, S.A., 2018, Water temperature in tributaries, off-channel features, and main channel of the lower Willamette River, northwestern Oregon, summers 2016 and 2017: U.S. Geological Survey Open-File Report 2018-1184, 33 p., accessed January 9, 2021, at https://doi.org/10.3133/ofr20181184.

Marine, K.R., and Cech, J.J., Jr., 2004, Effects of high water temperature on growth, smoltification, and predator avoidance in juvenile Sacramento River Chinook salmon: North American Journal of Fisheries Management, v. 24, no. 1, p. 198–210, accessed January 9, 2021, at https://doi.org/10.1577/M02-142.

McCullough, D.A., 1999, A review and synthesis of effects of alterations to the water temperature regime on freshwater life stages of salmonids, with special reference to Chinook salmon: U.S. Environmental Protection Agency, EPA 910-R-99-010, 279 p.

Mosley, M.P., 1983, Variability of water temperatures in the braided Ashley and Rakaia rivers: New Zealand Journal of Marine and Freshwater Research, v. 17, no. 3, p. 331–342, accessed January 9, 2021, at https://doi.org/10.1080/00288330.1983.9516007.

Myers, J., Busack, C., Rawding, D., Marshall, A., Teel, D., Van Doornik, D.M., and Maher, M.T., 2006, Historical population structure of Pacific salmonids in the Willamette River and lower Columbia River basins: U.S. Department of Commerce, National Oceanic and Atmospheric Administration technical memorandum NMFS-NWFSC-73, 311 p.

National Marine Fisheries Service, 1999a, Endangered and threatened species—Threatened status for three Chinook salmon evolutionarily significant units (ESUs) in Washington and Oregon, and endangered status for one Chinook salmon ESU in Washington: Federal Register, v. 64, no. 56, p. 14307–14328.

National Marine Fisheries Service, 1999b, Endangered and threatened species—Threatened status for two ESUs of chum salmon in Washington and Oregon, for two ESUs of steelhead in Washington and Oregon, and for Ozette Lake sockeye salmon in Washington—Rules: Federal Register, v. 64, no. 57, p. 14508–14517.

National Marine Fisheries Service, 2008, Willamette Basin biological opinion—Endangered Species Act section 7(a)(2) consultation: National Oceanic and Atmospheric Administration, Fisheries Log Number F/NWR/2000/02117 [variously paged], accessed November 30, 2020, at https://www.fisheries.noaa.gov/resource/document/consultation-willamette-river-basin-flood-control-project.

National Oceanic and Atmospheric Administration National Centers for Environmental Information, 2020, Climate at a Glance: Divisional Time Series, accessed November 16, 2020, at https://www.ncdc.noaa.gov/cag/

Olden, J.D., and Naiman, R.J., 2010, Incorporating thermal regimes into environmental flows assessments—Modifying dam operations to restore freshwater ecosystem integrity: Freshwater Biology, v. 55, no. 1, p. 86–107, accessed January 9, 2021, at https://doi.org/10.1111/j.1365-2427.2009.02179.x.

Oregon Department of Environmental Quality, 2006a, Willamette Basin Total Maximum Daily Load order memorandum: Oregon Department of Environmental Quality, accessed May 29, 2022, at https://www.oregon.gov/deq/FilterDocs/ordermemo.pdf.

Oregon Department of Environmental Quality, 2006b, Willamette Basin Total Maximum Daily Load program documents: Oregon Department of Environmental Quality, accessed May 29, 2022, at https://www.oregon.gov/deq/wq/tmdls/Pages/TMDLs-Willamette-Basin.aspx.

Oregon Department of Fish and Wildlife, The State of Oregon, and the National Oceanic and Atmospheric Administration, 2011, Upper Willamette River conservation and recovery plan for Chinook Salmon and Steelhead: Executive Summary, Oregon Department of Fish and Wildlife, accessed January 9, 2021, at https://www.dfw.state.or.us/fish/crp/upper_willamette_river_plan.asp.

Oregon Department of Fish and Wildlife and National Marine Fisheries Service, 2011, Upper Willamette River conservation and recovery plan for Chinook salmon and steelhead, FINAL—August 5, 2011: Oregon Department of Fish and Wildlife and the National Marine Fisheries Service Northwest Region, 462 p., accessed November 30, 2020, at https://repository.library.noaa.gov/view/noaa/15981.

Perry, R.W., J.M. Plumb, and C.W. Huntington, 2015, Using a laboratory-based growth model to estimate mass and temperature-dependent growth parameters across population of juvenile Chinook salmon: Transactions of the American Fisheries Society, v. 144, no. 2, p. 331–336, accessed January 9, 2021, at https://doi.org/10.1080/00028487.2014.996667.

Poole, G.C., and Berman, C.H., 2001, An ecological perspective on in-stream temperature—Natural heat dynamics and mechanisms of human-caused thermal degradation: Environmental Management, v. 27, no. 6, p. 787–802, accessed January 9, 2021, at https://doi.org/10.1007/s002670010188.

PRISM Climate Group, 2020, PRISM climate data: Corvallis, Prism Climate Group, Oregon State University website, accessed April 28, 2020, at http://www.prism.oregonstate.edu.

R Core Team, 2020, R—A language and environment for statistical computing—Vienna, Austria, R Foundation for Statistical Computing, accessed January 9, 2021, at https://www.R-project.org/.

Risley, J., Wallick, J.R., Waite, I., and Stonewall, A., 2010, Development of an environmental flow framework for the McKenzie River basin, Oregon: U.S. Geological Survey Scientific Investigations Report 2010-5016, 94 p., accessed January 9, 2021, at https://pubs.usgs.gov/sir/2010/5016/.

Risley, J.C., Wallick, J.R., Mangano, J.F., and Jones, K.L, 2012, An environmental streamflow assessment for the Santiam River Basin, Oregon: U.S. Geological Survey Open-File Report 2012-1133, 66 p., accessed January 14, 2021, at https://doi.org/10.3133/ofr20121133.

Rounds, S.A., and Buccola, N.B., 2015, Improved algorithms in the CE-QUAL-W2 water-quality model for blending dam releases to meet downstream water-temperature targets: U.S. Geological Survey Open-File Report 2015–1027, 36 p. [Also available at https://doi.org/10.3133/ofr20151027.]

Rounds, S.A., 2007, Temperature effects of point sources, riparian shading, and dam operations on the Willamette River, Oregon: U.S. Geological Survey Scientific Investigations Report 2007–5185, 34 p. [Also available at https://doi.org/10.3133/sir20075185.]

Rounds, S.A., 2010, Thermal effects of dams in the Willamette River Basin, Oregon: U.S. Geological Survey Scientific Investigations Report 2010–5153, 64 p. [Also available at https://doi.org/10.3133/sir20105153.]

Rounds, S.A., and Stratton Garvin, L.E., 2022, Tracking heat in the Willamette River system, Oregon: U.S. Geological Survey Scientific Investigations Report 2022–5006, 47 p. [Also available at https://doi.org/10.3133/sir20225006.]

Sedell, J.R., and Froggatt, J.L., 1984, Importance of streamside forests to large rivers—The isolation of the Willamette River, Oregon, U.S.A. from its floodplain by snagging and streamside forest removal: SIL Proceedings, 1922–2010, v. 22, no. 3, p. 1828–1834, accessed January 9, 2021, at https://doi.org/10.1080/03680770.1983.11897581.

Smith, C.D., Mangano, J.F., and Rounds, S.A., 2020, Temperature and water-quality diversity and the effects of surface-water connection in off-channel features of the Willamette River, Oregon, 2015–16: U.S. Geological Survey Scientific Investigations Report 2020–5068, 70 p., accessed January 9, 2021, at https://doi.org/10.3133/sir20205068.

Steel, E.A., Beechie, T.J., Torgersen, C.E., and Fullerton, A.H., 2017, Envisioning, quantifying, and managing thermal regimes on river networks: Bioscience, v. 67, no. 6, p. 506–522, accessed January 9, 2021, at https://doi.org/10.1093/biosci/bix047.

Stratton Garvin, L.E., and Rounds, S.A., 2022, CE-QUAL-W2 models for the Willamette River and major tributaries below U.S. Army Corps of Engineers dams—2011, 2015, and 2016: U.S. Geological Survey Data Release, https://doi.org/10.5066/P908DXKH.

Stratton Garvin, L.E., Rounds, S.A., Buccola, N.L., 2022a, Estimating stream temperature in the Willamette River Basin, northwestern Oregon—A regression-based approach: U.S. Geological Survey Scientific Investigations Report 2021–5022, 40 p., accessed May 29, 2022, at https://doi.org/10.3133/sir20215022.

Stratton Garvin, L.E., Rounds, S.A., and Buccola, N.L., 2022b, Updates to models of streamflow and water temperature for 2011, 2015, and 2016 in rivers of the Willamette River Basin, Oregon: U.S. Geological Survey Open-File Report 2022–1017, 73 p., accessed May 29, 2022, at https://doi.org/10.3133/ofr20221017.

Sullivan, A.B., and Rounds, S.A., 2004, Modeling streamflow and water temperature in the North Santiam and Santiam Rivers, Oregon, 2001–02: U.S. Geological Survey Scientific Investigations Report 2004–5001, 44 p. [Also available at https://doi.org/10.3133/sir20045001.]

Tague, C., and Grant, G.E., 2004, A geological framework for interpreting the low-flow regimes of Cascade streams, Willamette River Basin, Oregon: Water Resources Research, v. 40, no. 4, accessed January 9, 2021, at https://doi.org/10.1029/2003WR002629.

Tague, C., Farrell, M., Grant, G., Lewis, S., and Rey, S., 2007, Hydrogeologic controls on summer stream temperatures in the McKenzie River Basin, Oregon: Hydrological Processes, v. 21, no. 24, p. 3288–3300, accessed January 9, 2021, at https://doi.org/10.1002/hyp.6538.

Torgersen, C.E., Ebersole, J.L., and Keenan, D.M., 2012, Primer for identifying cold-water refuges to protect and restore thermal diversity in riverine landscapes: U.S. Environmental Protection Agency, EPA 910-C-12- 001, 91 p., accessed May 29, 2022, at https://pubs.er.usgs.gov/publication/70037945.

U.S. Army Corps of Engineers, 2020, DataQuery 2.0: U.S. Army Corps of Engineers, accessed November 16, 2020, at https://pweb.crohms.org/dd/common/dataquery/www/.

U.S. Geological Survey, 2020, National Water Information System: U.S. Geological Survey, web interface, accessed November 10, 2020, at https://doi.org/10.5066/F7P55KJN.

Vannote, R.L., Minshall, G.W., Cummins, K.W., Sedell, J.R., and Cushing, C.E., 1980, The river continuum concept: Canadian Journal of Fisheries and Aquatic Sciences, v. 37, no. 1, p. 130–137, accessed January 9, 2021, at https://doi.org/10.1139/f80-017.

Wallick, J.R., Bach, L.B., Keith, M.K., Olson, M., Mangano, J.F., and Jones, K.L., 2018, Monitoring framework for evaluating hydrogeomorphic and vegetation responses to environmental flows in the Middle Fork Willamette, McKenzie, and Santiam River Basins, Oregon: U.S. Geological Survey Open-File Report 2018–1157, 66 p., accessed January 9, 2021, at https://doi.org/10.3133/ofr20181157.

Wallick, J.R., Grant, G.E., Lancaster, S.T., Bolte, J.P., and Denlinger, R.P., 2007, Patterns and controls on historical channel change in the Willamette River, Oregon, *in* Gupta, A.V., ed., Large rivers—Geomorphology and management: Chichester, United Kingdom, Wiley, p. 491–516.

Wallick, J.R., Jones, K.L., O'Connor, J.E., Keith, M.K., Hulse, D., and Gregory, S.V., 2013, Geomorphic and vegetation processes of the Willamette River floodplain, Oregon—Current understanding and unanswered questions: U.S. Geological Survey Open-File Report 2013–1246, 70 p., accessed January 9, 2021, at https://doi.org/10.3133/ofr20131246.

Webb, B.W., Hannah, D.M., Moore, R.D., Brown, L.E., and Nobilis, F., 2008, Recent advances in stream and river temperature research: Hydrological Processes, v. 22, no. 7, p. 902–918, accessed January 9, 2021, at https://doi.org/10.1002/hyp.6994.

Wentz, D.A., Bonn, B.A., Carpenter, K.D., Hinkle, S.R., Janet, M.L., Rinella, F.A., Uhrich, M.A., Waite, I.R., Laenen, A., and Bencala, K.E., 1998, Water quality in the Willamette Basin, Oregon, 1991-95: U.S. Geological Survey Circular 1161, 34 p., accessed January 9, 2021, at https://pubs.usgs.gov/circ/circ1161.

Wetzel, R.G., 2001, Limnology—Lake and river ecosystems (3rd ed.): San Francisco, Academic Press, 1006 p., accessed January 9, 2021, at https://doi.org/10.1016/C2009-0-02112- 6.

Wells, S.A., 2019, CE-QUAL-W2—A two-dimensional, laterally-averaged, hydrodynamic and water quality model, Version 4.2: Portland, Oregon, Department of Civil and Environmental Engineering, Portland State University, [variously paged.]

White, J.S., Peterson, J.T., Stratton Garvin, L.E., Kock, T.J., and Wallick, J.R., 2022, Assessment of habitat availability for juvenile Chinook salmon (*Oncorhynchus tshawytscha*) and steelhead (*O. mykiss*) in the Willamette River, Oregon: U.S. Geological Survey Scientific Investigations Report 2022–5034, 44 p. [Also available at https://doi.org/10.3133/sir20225034.]

Appendix 1. Model Evaluation and Applications

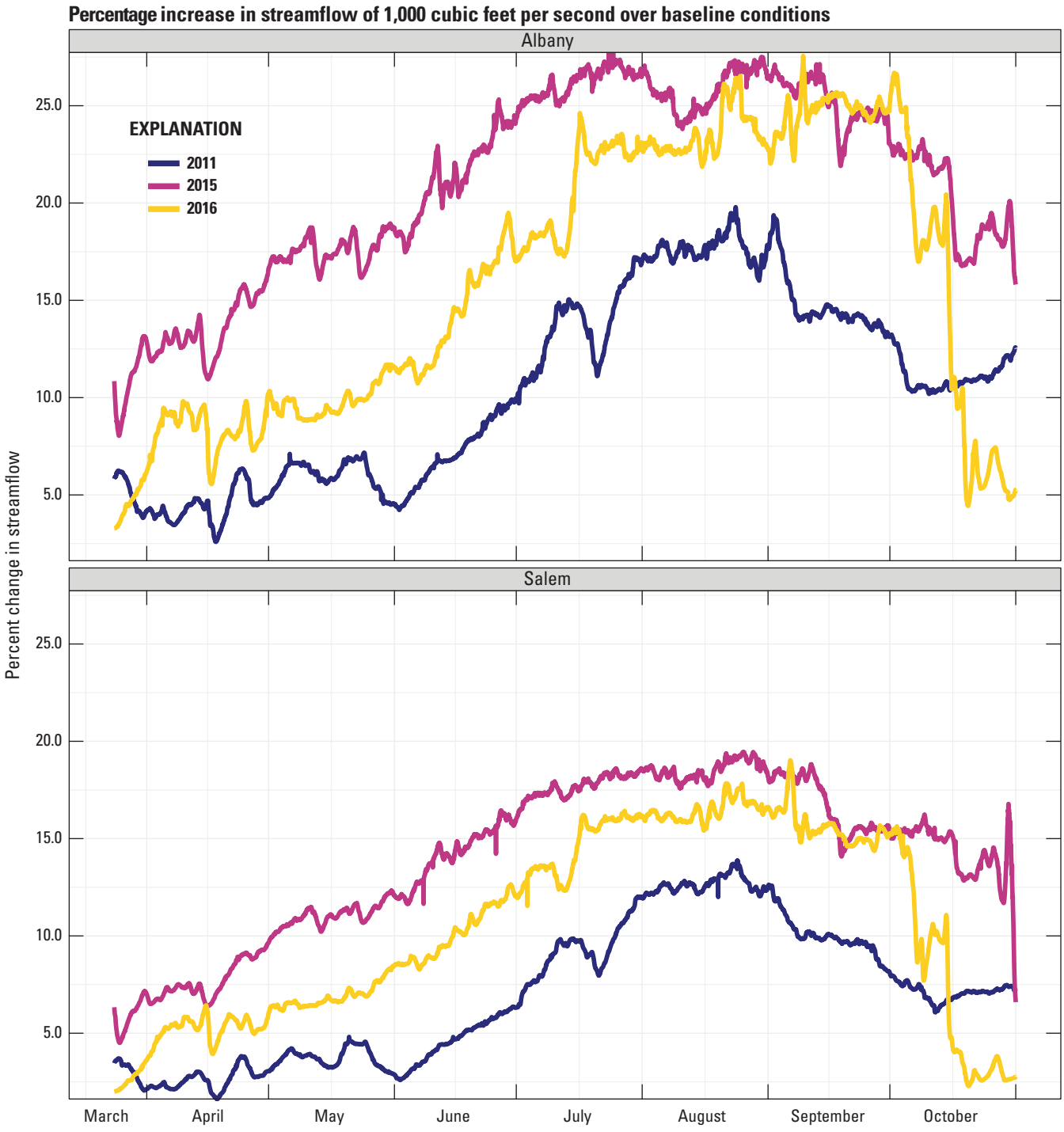

Figure 1.1. Graphs showing the percent increase in streamflow from baseline conditions with the addition of 1,000 cubic feet per second for the entire model period in 2011, 2015, and 2016 at U.S. Geological Survey station 14174000 (Willamette River at Albany) (top panel) and U.S. Geological Survey station 14191000 (Willamette River at Salem, northwestern Oregon).

Publishing support provided by the
U.S. Geological Survey Science Publishing Network
Tacoma Publishing Service Center
For more information concerning the research in this report, contact the
Director, Oregon Water Science Center
U.S. Geological Survey
2130 SW 5th Avenue
Portland, Oregon 97201
https://www.usgs.gov/centers/or-water

USGS

Stratton Garvin and Rounds—**Thermal Landscape of Willamette River—Patterns and Controls on Stream Temperature**—SIR 2022–5035

ISSN 2328-0328 (online)
https://doi.org/10.3133/sir20225035